2019

Analog Least Mean Square Loop for Self-Interference Cancellation in In-band Full-duplex Systems

Anh Tuyen Le
AnhTuyen.Le@student.uts.edu.au

Le Chung Tran
University of Wollongong, lctran@uow.edu.au

Xiaojing Huang
huang@uow.edu.au

Y. Jay Guo

Analog Least Mean Square Loop for Self-Interference Cancellation in In-band Full-duplex Systems

Abstract

Analog Least Mean Square (ALMS) loop is a promising method to cancel self-interference (SI) in in-band full-duplex (IBFD) systems. In this talk, the steady state analyses of the residual SI powers in both analog and digital domains are derived in frequency domain. It is proved that the ALMS loop amplifies the frequency components of the residual SI at the edges of the signal spectrum in the analog domain, but the matched filter in the receiver chain reduces this effect. This results in a significant improvement of the interference suppression ratio in the digital domain before information data detection. The lower bounds of the interference suppression ratio given by the ALMS loop in both analog and digital domains are then addressed. These lower bounds are proved to be joint effects of the loop gain, tap delay, number of taps, and transmitted signal properties. The discovered relationship among these parameters allows the flexibility in choosing appropriate parameters when designing the IBFD systems under given constraints. Finally, the effects of I/Q imbalance in the ALMS loop and the upper bound of the degradation on SI cancellation performance are then investigated. The degradation is proved to be insignificant even under severe conditions of I/Q imbalance. The upper bound of the degradation provides an essential reference for the system design.

Keywords

least, mean, square, analog, loop, self-interference, systems, cancellation, in-band, full-duplex

Disciplines

Engineering | Science and Technology Studies

Publication Details

A. Le, L. Tran, X. Huang & Y. Guo, "Analog Least Mean Square Loop for Self-Interference Cancellation in In-band Full-duplex Systems," in IEEE International Conference on Signal Processing and Communications Systems (ICSPCS 2019), 2019,

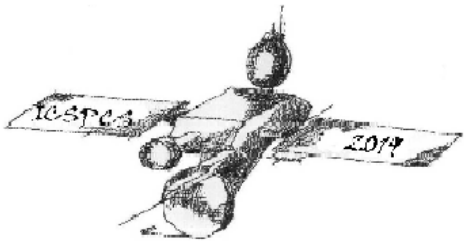

Analog Least Mean Square Loop for
Self-Interference Cancellation in In-band Full-duplex Systems

Presenter: **Dr. Le Chung Tran**

Anh Tuyen Le[1], Le Chung Tran[2], Xiaojing Huang[1] and Y. Jay Guo[1]

[1]University of Technology Sydney, Ultimo, NSW, 2007, Australia
[2] University of Wollongong, Wollongong, NSW, 2522, Australia

Table of contents

Full-duplex Communications

A new scheme that allows simultaneous transmit and receive on the same frequency band:

- Double spectral efficiency
- Solve hidden-terminal problem
- Reduce round-trip latency

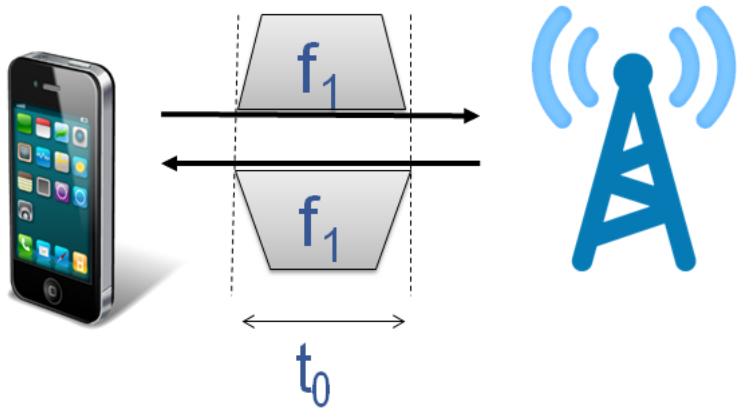

Fig. 1. Full-duplex operation.

Self-interference Problem

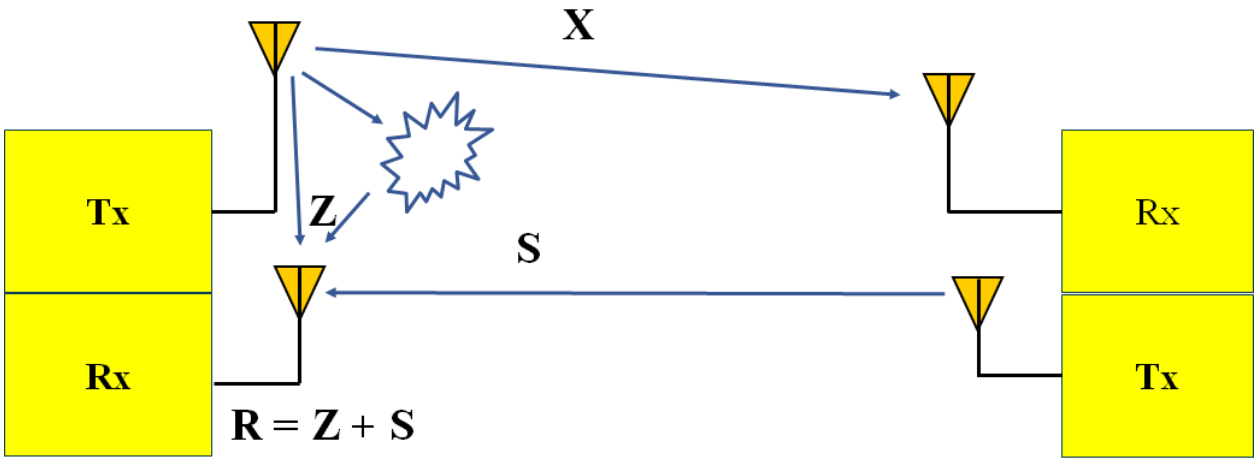

Fig. 2. Self-interference problem.

- Z is the self-interference (SI)
- Z is the same as S but $Z \gg S$
- Self-interference cancellation (SIC): Reduce Z to below noise floor

Self-interference Cancellation

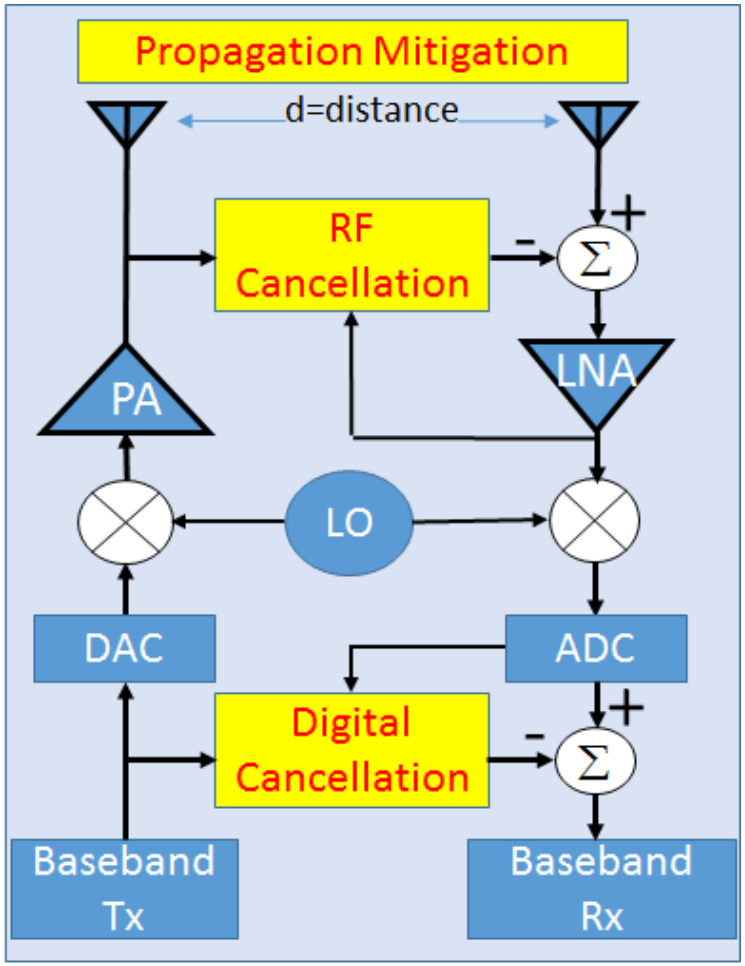

Fig. 3. SIC approaches.

- Propagation domain: Mitigate the level of SI at the receive antenna;
- RF domain cancellation: Generate a signal which mimics the SI to cancel it at the input of the receiver;
- Digital domain cancellation: Employ the transmit baseband signal and channel state information to cancel the digitized residual SI.

Self-Interference Mitigation Techniques

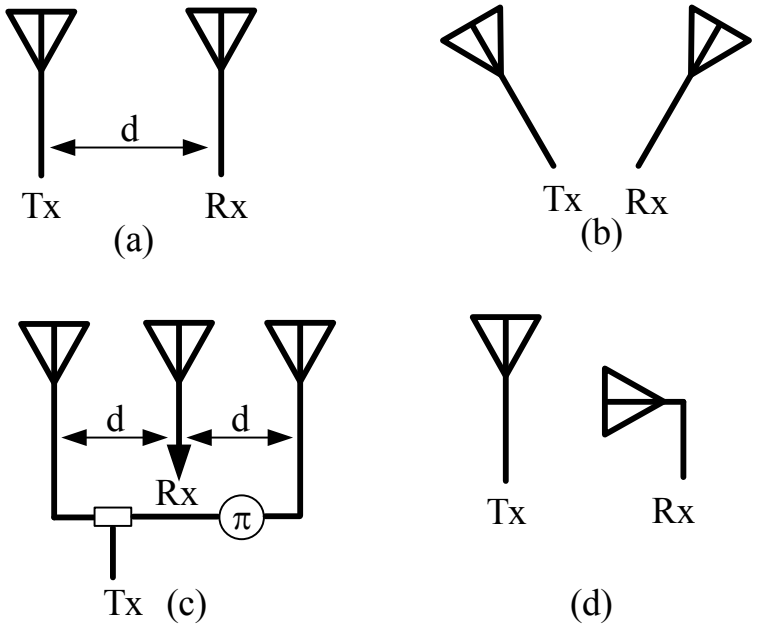

Fig. 4. Propagation domain approaches.

- (a) Physical separation
- (b) Spatial/beam separation
- (c) Antiphase control
- (d) Cross polarization

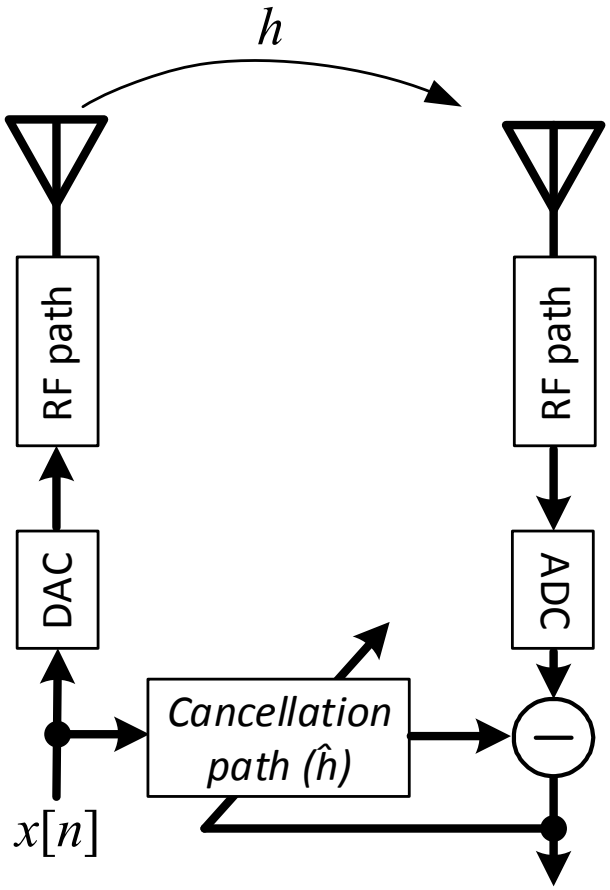

Fig. 5. Digital domain cancellation approaches.

- Least Mean Square algorithm
- Blind Source Separation algorithm

Self-Interference Mitigation Techniques

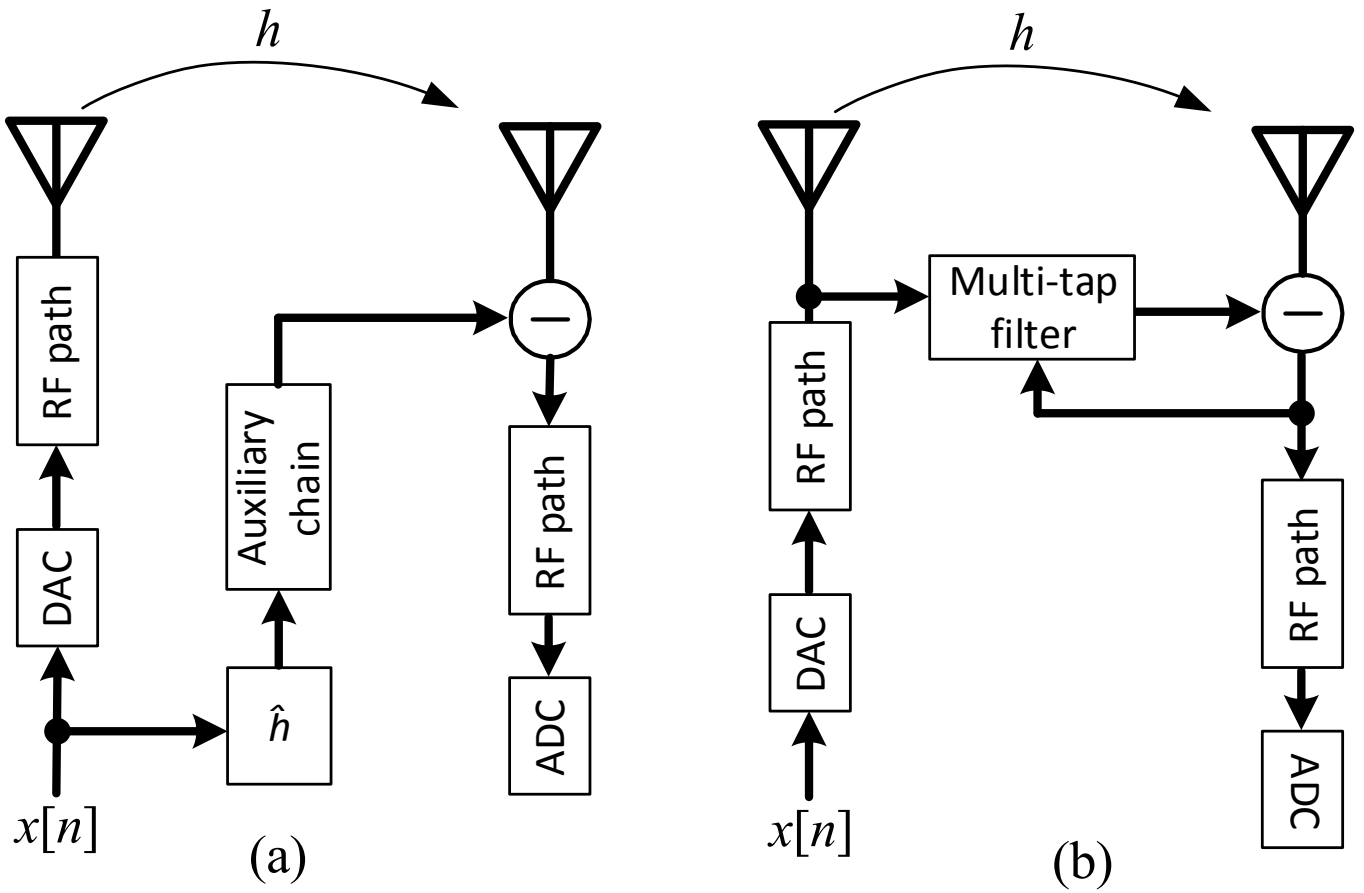

Fig. 6. Analog domain cancellation: (a) Additional Transmit chain (b) Multi-tap adaptive filter.

Multi-tap Adaptive Canceller

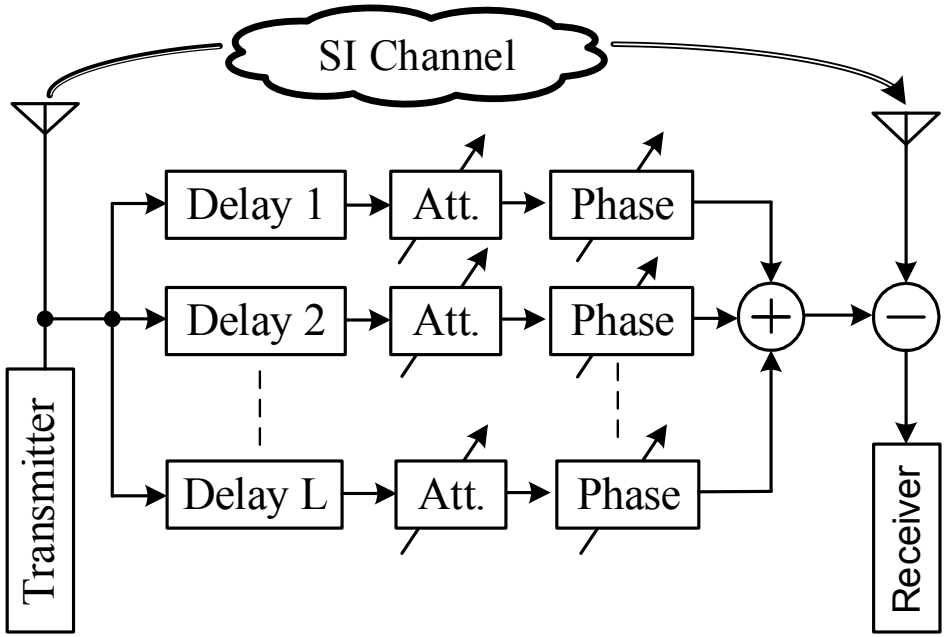

Fig. 7. SIC approaches.

Based on the assumption that the SI channel is a multi-tap filter. This structure has great advantages:

- Able to cancel the SI with high-order components of transmitted signal and transmitter noise;
- Suitable for wide-band applications;
- Adaptable with the change of surrounding environment.

Multi-tap Adaptive Canceller (continue)

Some typical examples of multi-tap cancellers are compared in Table 1.

	# of taps	Delay line	Tap weight control	ISR (dB)	Bandwidth (MHz)
Bharadia et al.	8	Microstrip trace	FPGA	45	80
Huusari et al.	2	Anaren IC	Down converter + Integrator	33	20
Kolodziej et al.	4	Coaxial cable	FPGA	21.6	20
Liyuan et al.	8	Microstrip trace	FPGA	38	20

- Most of the cancellers require digital signal processing (DSP) and channel state information (CSI) to synthesize tap weight coefficients;
- The involvements of DSP and CSI lead to significant complexity when applying for IBFD MIMO systems.

ALMS Loop

Fundamental:

- Based on least mean square algorithm to minimize the residual SI;
- The residual signal is amplified and looped-back to update the weighting coefficients;
- Resistor-capacitor low-pass filters are used to synthesize the weighting coefficients;

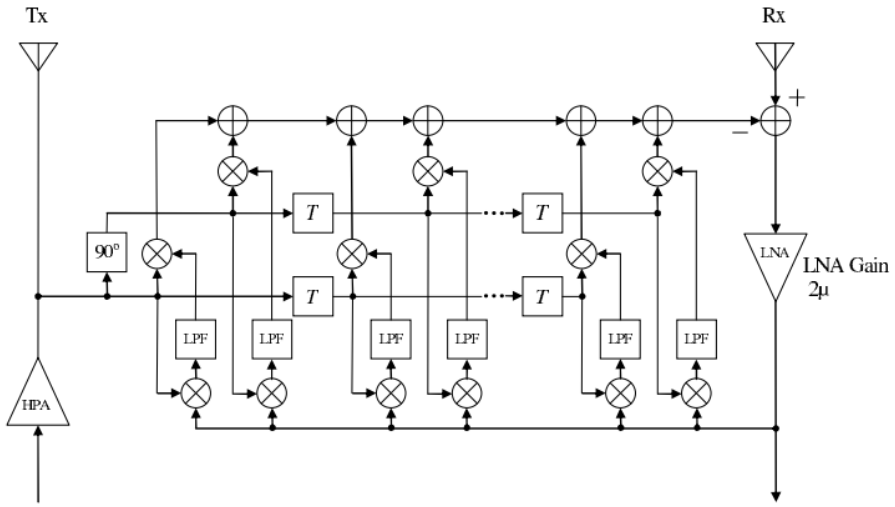

Fig. 8. The ALMS loop proposed in [1].

[1] X. Huang and J. Guo, "Radio frequency self-interference cancellation with analog least mean square loop", IEEE Trans. Microw. Theory Tech., vol. 65, no. 9, pp. 3336 - 3350, 2017.

Operations of ALMS Loop

Signal models:

- Tx signal: $x(t) = Re\left\{X(t)e^{j2\pi f_c t}\right\}$

$$X(t) = V_X \sum_{i=-\infty}^{\infty} a_i p(t - iT_s)$$

- SI signal:

$$z(t) = Re\left\{\sum_{l=0}^{L-1} h_l^* X(t - lT_d))e^{j2\pi f_c t}\right\}$$

- Cancellation signal $y(t) =$

$$Re\left\{\sum_{l=0}^{L-1} w_l^*(t)X(t - lT_d)e^{j2\pi f_c(t-lT_d)}\right\}$$

- Received signal $r(t) = s(t) + z(t) + n(t)$
- After SI cancellation $d(t) = r(t) - y(t)$

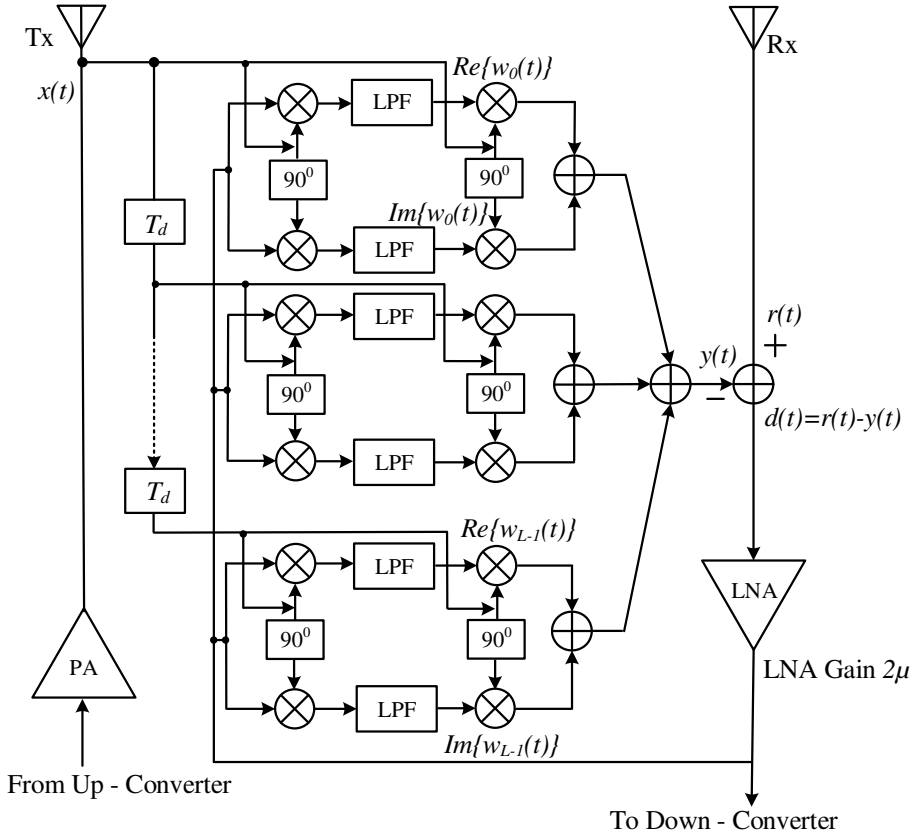

Fig. 9. The ALMS loop proposed in [1].

Operations of ALMS Loop

- The weighting coefficient at l-th tap [1,Eq.(5)]:

$$w_l(t) = \frac{2\mu\alpha}{K_1 K_2} \int_0^t e^{-\alpha(t-\tau)}[r(\tau) - y(\tau)]X(\tau - lT_d)e^{j2\pi f_c(\tau - lT_d)}d\tau \tag{1}$$

- The residual SI signal $v(t) = z(t) - y(t)$:

$$v(t) = Re\Big\{ \sum_{l=0}^{L-1} [h_l - w_l(t)e^{j2\pi f_c l T_d}]^* X(t - lT_d)e^{j2\pi f_c t} \Big\} \tag{2}$$

- The weighting error function: $u_l(t) = h_l - w_l(t)e^{j2\pi f_c l T_d}$ **represents the performance of the ALMS loop!**
- Its expectation [1, Eq.(13)]

$$\bar{u}_l(t) = h_l - \frac{\mu\alpha}{K_1 K_2} \int_0^t e^{-\alpha(t-\tau)} \sum_{l'=0}^{L-1} \bar{u}_{l'}(\tau)\Phi_{XX}(\tau; (l - l')T_s)d\tau \tag{3}$$

ALMS Loop - Earlier Results

- Expected weighting error function

$$\bar{u}_l(t) \approx h_l \frac{1+\mu A^2 e^{-(1+\mu A^2)\alpha t}}{1+\mu A^2} e^{-\mu A^2 \alpha T_s \beta/\pi^2 \sin \frac{2\pi}{T_s} t} \quad (4)$$

- Variation of $\bar{u}_l(t)$ (w/wo cyclostationary part)

$$\tilde{u}_l(t) \approx h_l \frac{1+\mu A^2 e^{-(1+\mu A^2)\alpha t}}{1+\mu A^2} \left(e^{-\mu A^2 \alpha T_s \beta/\pi^2 \sin \frac{2\pi}{T_s} t} - 1 \right) \quad (5)$$

- Averaged residual power (ignoring cyclostationary part, no modeling error) $P_{RI} \approx \frac{1}{(1+\mu A^2)^2} \frac{A^2}{2} \sum_{l=0}^{L-1} |h_l|^2$
- Averaged SI power $P_I = \frac{A^2}{2} \sum_{l=0}^{L-1} |h_l|^2$
- Interference Suppression Ratio [1, p.6] $ISR = \frac{P_{RI}}{P_I} \approx \frac{1}{(1+\mu A^2)^2}$

ALMS Loop-Earlier Results

- Irreducible SI power (based on (5))

$$P_{II} = \frac{A^2}{2} \sum_{l=0}^{L-1} \frac{1}{T_s} \int_0^{T_s} |\tilde{u}_l(t)|^2 dt = \frac{A^2}{2} \sum_{l=0}^{L-1} |h_l|^2 \left(\alpha T_s \frac{\beta}{\pi^2} \right)^2 \quad (6)$$

- Interference suppression lower bound (ISRLB)

$$ISRLB = \frac{P_{II}}{P_I} = \frac{1}{2} \left(\alpha T_s \frac{\beta}{\pi^2} \right)^2 \quad (7)$$

- Normalised modeling error [1, Eq.(24)]

$$\epsilon^2 = \frac{1}{K_1 K_2} \bar{E}\{ | \int_{-\infty}^{\infty} h^*(\tau') X(t-\tau') d\tau' - \sum_{l=0}^{L-1} h_l^* X(t-lT_s) |^2 \}$$
$$= \int_{-\infty}^{\infty} \int_{-\infty}^{\infty} h^*(\tau) h^*(\tau') \Phi(\tau - \tau') d\tau' d\tau - \mathbf{h}^H \Phi \mathbf{h} \quad (8)$$

ALMS Loop-Earlier Results

- In the macro scale (steady state) analysis, both ensemble expectation and time averaging are used.
- Normalised RI power converges to (see Fig. 12)

$$P_{RI} = \epsilon^2 + \mathbf{h}^H \mathbf{Q} \text{diag}\{\frac{\lambda_l}{(1+\mu\lambda_l)^2}\}\mathbf{Q}^{-1}\mathbf{h} \tag{9}$$

- Normalised SI power converges to

$$P_I = \epsilon^2 + \mathbf{h}^H \Phi \mathbf{h} \tag{10}$$

- The interference suppression ratio is determined as:

$$ISR = \frac{P_{RI}}{P_I} = \frac{\epsilon^2 + \mathbf{h}^H \mathbf{Q} \text{diag}\{\frac{\lambda_l}{(1+\mu\lambda_l)^2}\}\mathbf{Q}^{-1}\mathbf{h}}{\epsilon^2 + \mathbf{h}^H \mathbf{\Phi} \mathbf{h}} \tag{11}$$

ALMS Loop-Earlier Results

- λ_l are eigenvalues of the normalised autocorrelation matrix

$$\mathbf{\Phi} = \begin{bmatrix} \Phi(0) & \Phi(-T_d) & \dots & \Phi(-(L-1)T_d) \\ \Phi(T_d) & \Phi(0) & \dots & \Phi(-(L-2)T_d) \\ \dots & \dots & \dots & \dots \\ \Phi((L-1)T_d) & \Phi((L-2)T_d) & \dots & \Phi(0) \end{bmatrix} \tag{12}$$

- Normalized autocorrelation function

$$\begin{aligned} \Phi(\tau) &= \frac{1}{K_1 K_2} \bar{E}\{X^*(t)X(t-\tau)\} \\ &= \frac{1}{K_1 K_2 T_s} \int_0^{T_s} E\{X^*(t)X(t-\tau)\} \\ &= \frac{1}{K_1 K_2 T_s} \int_{-\infty}^{\infty} p^*(t)p(t-\tau)d\tau \end{aligned} \tag{13}$$

ALMS Loop-Earlier Results

- In the micro scale, communication signal can be seen as a wide-sense cyclostationary process.
- This cyclostationary property leads to variation in the weighting error function and hence irreducible self-interference.
- $ISR \approx \frac{1}{(1+\mu A^2)^2} \Rightarrow$ From the expectation of ISR, determining the loop gain μA^2 of the ALMS loop
- $ISRLB \approx \frac{1}{2}\left(\alpha T_s \frac{\beta}{\pi^2}\right)^2$.
  $\Rightarrow$ Roll-off factor of the pusle shaping filter β affects the ISRLB.
  $\Rightarrow$ From the expectation of ISRLB, determining the decay constant α of the LPF

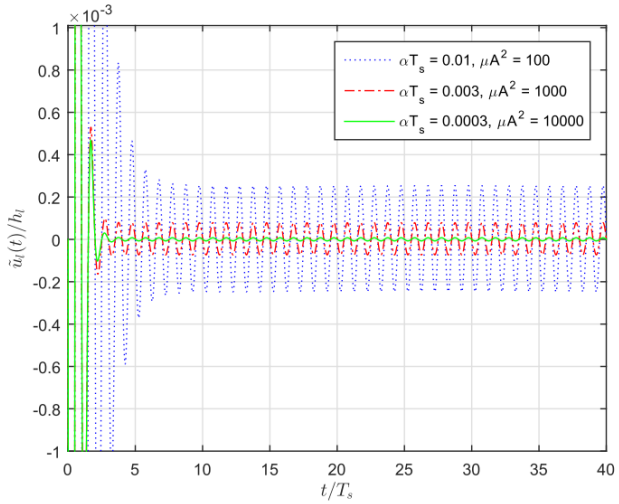

Fig. 10. Normalized weight error variation.

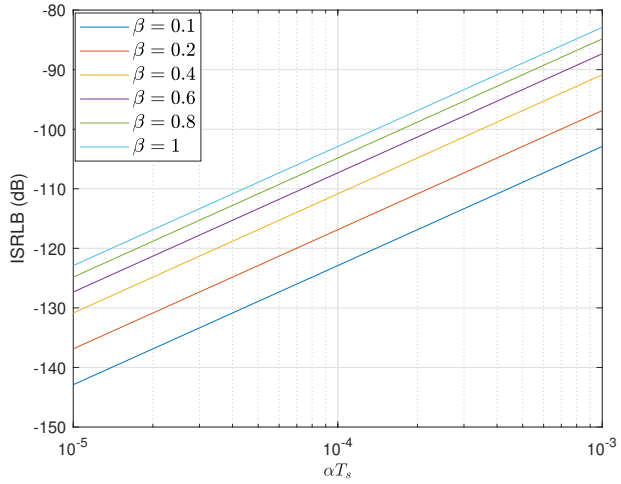

Fig. 11. ISR lower bounds.

ALMS Loop - Earlier Results

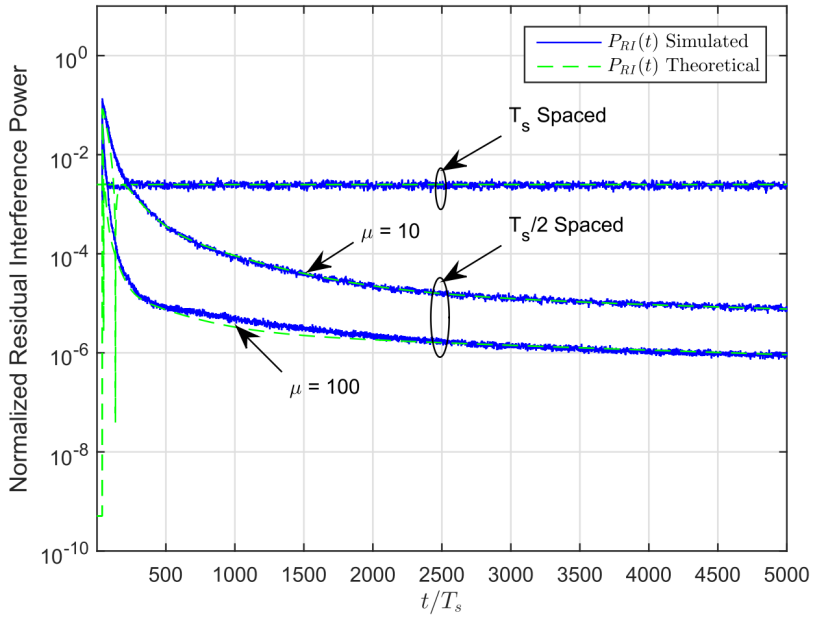

Fig. 12. Residual SI power [1, Fig.10].

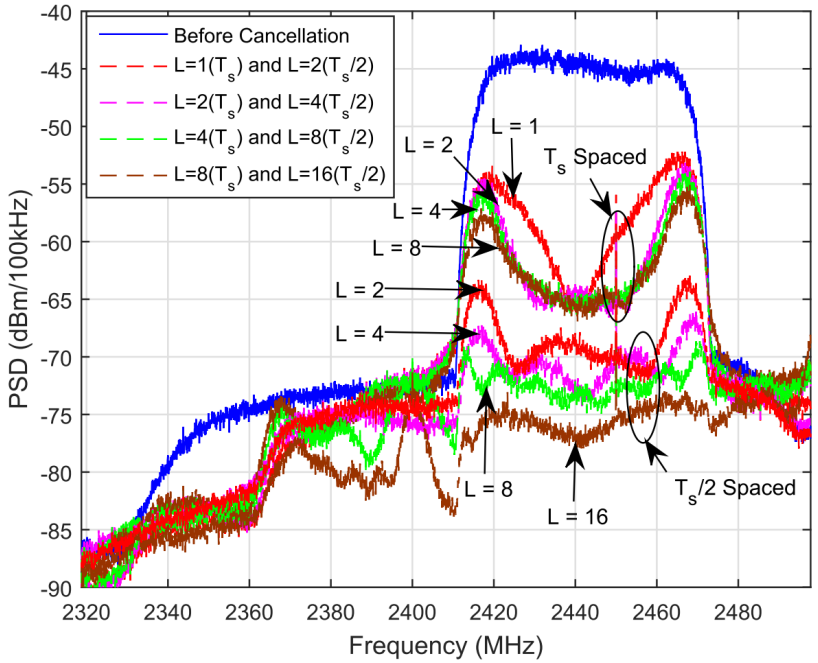

Fig. 13. Measured PSDs of SI and residual SI [1, Fig.13].

- $T_s/2$ spacing is better

- $(L = 2, T_s/2)$ better than $(L = 8, T_s)$
- $T_d = T_s/2$ provides 26-33 dB
- M-shaped spectrum

Research Aims and Objectives

Aims: Investigate the behavior of the ALMS loop and adopt it in different IBFD applications.

Objectives:

- ALMS loop with different transmitted signal properties
- The performance bounds of the ALMS loop
- ALMS loop with hardware impairment
- ALMS loop for IBFD MIMO systems
- Hardware implementation of the ALMS loop.

Single Carrier vs. Multi Carrier Signalling

- ALMS loop is evaluated with both single carrier and multi carrier signallings.
- Generalized weighting error function is expressed as [J1, Eq.(6)]:

$$\bar{u}_l(t) = h_l - \frac{\mu\alpha}{K_1 K_2} \int_0^t e^{-\alpha(t-\tau)} \sum_{l'=0}^{L-1} \bar{u}_{l'}(\tau)\Phi(\tau, (l-l')T_d)d\tau. \quad (14)$$

- Solution of the weighting error function can be found if the autocorrelation function satisfies $\Phi(\tau, (l-l')T_d) = 0$ for $l \neq l'$.
- Generalized solution for the weighting error function is [J1, Eq.(14)]:

$$\bar{u}_l(t) = \left[h_l \frac{1+\mu A^2 e^{-\alpha(1+\mu A^2)t}}{1+\mu A^2}\right] e^{-\mu A^2 \alpha q(t)} \quad (15)$$

where $q(t) = \int_0^t \left[\tilde{\Phi}(\tau, 0) - 1\right] d\tau$.

Single Carrier vs. Multi Carrier Signalling

- Interference suppression ratio lower bound

$$ISRLB = \frac{P_{II}}{P_I} = \frac{P_I \frac{1}{T}\int_0^T [\alpha q(t)]^2 dt}{P_I} = \frac{1}{T}\int_0^T [\alpha q(t)]^2 dt$$

- Single carrier systems [J1] (see (7)): $ISRLB_s = \frac{1}{2}\left(\alpha T_s \frac{\beta_s}{\pi^2}\right)^2$
- Multi-carrier systems [J1]

$$ISRLB_o = \frac{\alpha^2 T_o^2 \beta_o^2}{(4-\beta_o)^2(1+\beta_o)^2}\left\{\frac{25}{12}(1-\beta_o)^2 + \frac{5\beta_o}{16\pi^2}(81-55\beta_o)\right\}$$

Findings:

- ALMS loop performs well with both single carrier and multi carrier signallings.
- The weighting error function in the OFDM system varies more significantly due to longer symbol period.

.

Single Carrier vs. Multi Carrier Signalling (continue)

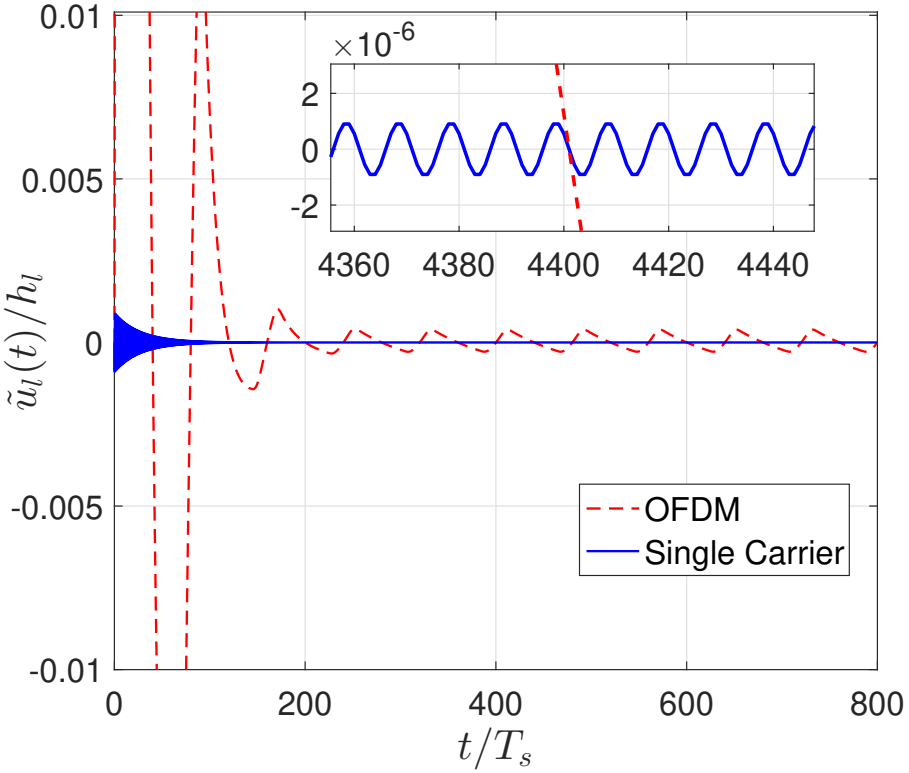

Fig. 14. Normalized weight error variations.

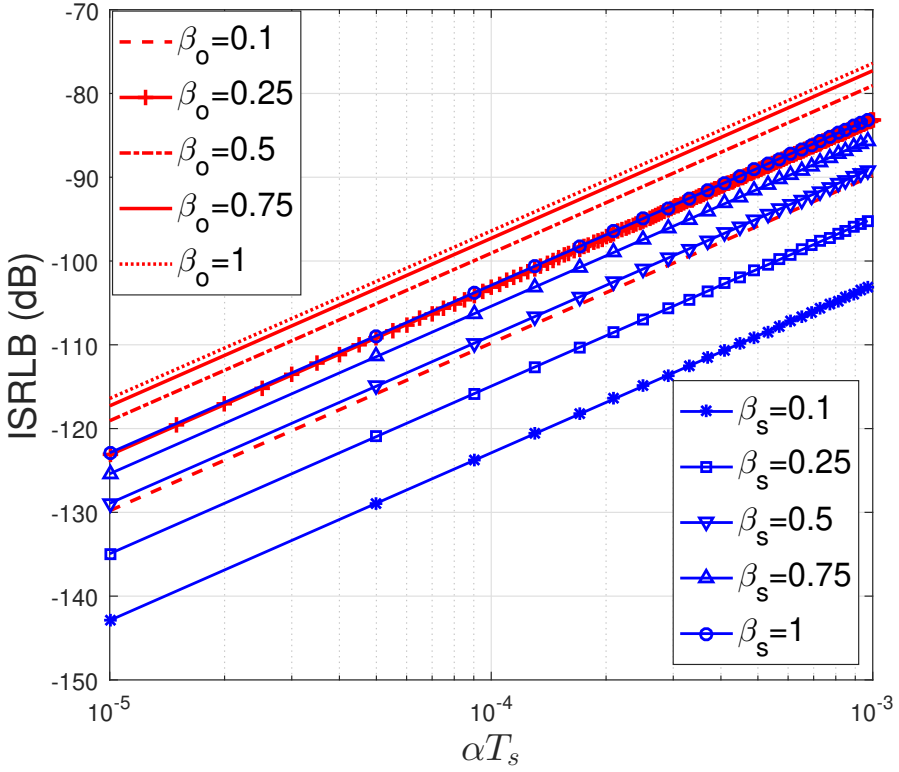

Fig. 15. Irreducible interference suppression ratio lower bounds.

Outcomes: VTC 2017 [C1] & IEEE Commun. Lett. 2017 [J1]

Deterministic Signal

- FD is applied in SAR (Synthetic Aperture Radar) [2]
- Chirp signal is periodically transmitted ($k_r = B/T$ chirp rate)

$$X(t) = \sum_{l=-\infty}^{\infty} V_X P(t - lT) \tag{16}$$

$$P(t) = \text{rect}(\frac{t}{T}) e^{j\pi k_r t^2}.$$

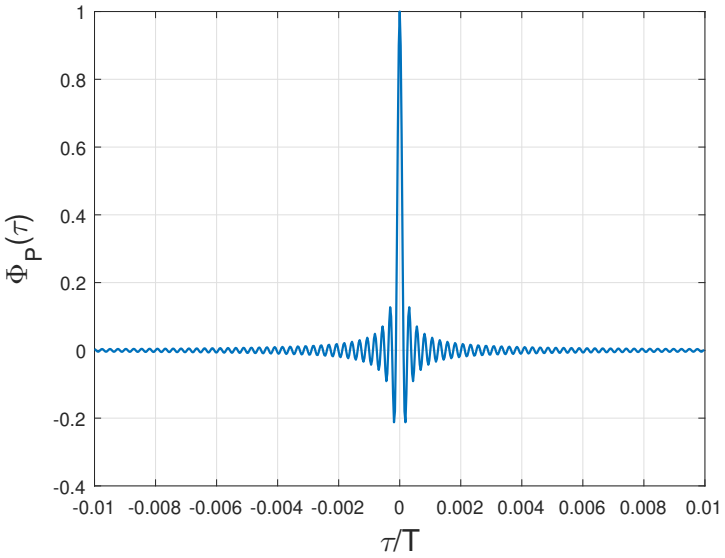

Fig. 16. The autocorrelation function of $P(t)$ with chirp rate $k_r = 2.5 \times 10^{12}$.

- Autocorrelation of $X(t)$, $\Phi(\tau)$, is a periodical function with the period T: $\Phi(\tau) = \sum_{l=-\infty}^{\infty} A^2 \Phi_P(\tau + lT)$
- $\Phi_P(\tau) = \frac{T-|\tau|}{T} \text{sinc}(\pi k_r \tau (T - |\tau|))$

[2] Y. Nan, X. Huang and Y. J. Guo, "Generalized Continuous Wave Synthetic Aperture Radar for High Resolution and Wide Swath Remote Sensing," in IEEE Trans. Geosci. Remote Sens, Dec. 2018.

Deterministic Signal

From the equation of the weighting error function [C2, Eq.(17)]

$$\bar{\bar{\mathbf{u}}}(t) = \mathbf{h} - \mu\alpha \int_0^t e^{-\alpha(t-\tau)} \mathbf{\Phi} \bar{\bar{\mathbf{u}}}(\tau) d\tau \tag{17}$$

(17) can be solved if the ALMS loop satisfies two conditions:

$$\begin{cases} T_d = \frac{1}{nk_rT} & \text{for } n = 1, 2, \cdots \\ (L-1)T_d \leqslant T \end{cases} \tag{18}$$

$\Rightarrow$ (18) is the suggestion for the design of ALMS loop in FD SAR.

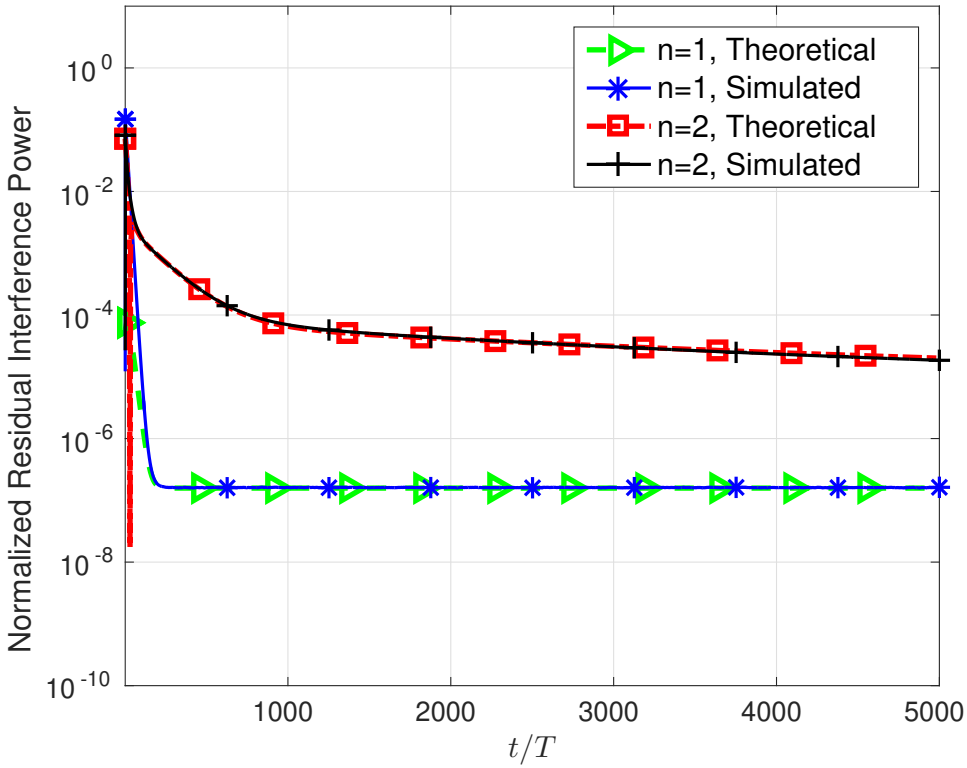

Fig. 17. The residual SI powers for $T_d = 1/nk_rT$, with $n = 1, 2$ and $L = 4, 8$ respectively.

Deterministic Signal

- In FD SAR with deterministic transmitted signals, ALMS loop behaves similarly as in a FD communication system with random transmitted signals.
- The weighting error functions $\bar{\bar{\mathbf{u}}}(t)$ converges to $\mathbf{Q}\text{diag}\left\{\frac{1}{1+\mu\lambda_l}\right\}\mathbf{Q}^{-1}\mathbf{h}$ when $t \rightarrow \infty$.
- Convergence speed is driven by the loop gain μA^2 and the LPF parameter α.
- The above analyses are valid when the tap delay $T_d \leqslant 1/B$ and the number of taps L, i.e., $(L-1)T_d \leqslant T$. These conditions are essential for practical system design.
- The ALMS loop can be used for deterministic signal. Outcome: A paper published in VTC 2018 [C2]

From the spectrum result in [1]:

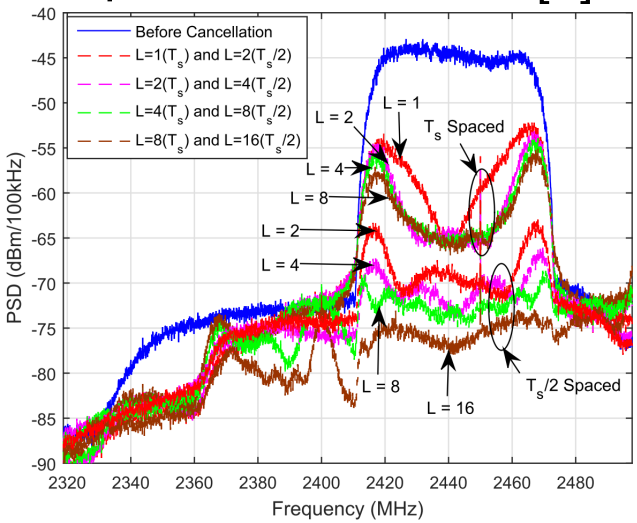

Fig. 18. PSDs of SI and residual SI.

- Peaks appearing at the edge of residual SI spectrum. WHY?
- Performance bounds in analog and digital domain?

From the spectrum result in [1]:

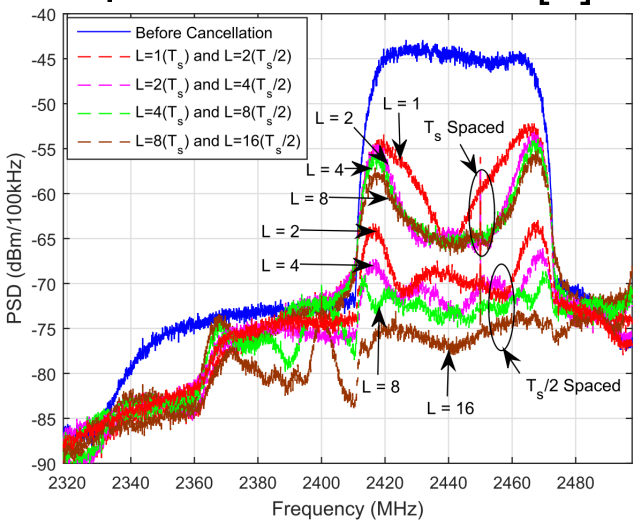

Fig. 18. PSDs of SI and residual SI.

- Peaks appearing at the edge of residual SI spectrum. WHY?
- Performance bounds in analog and digital domain?

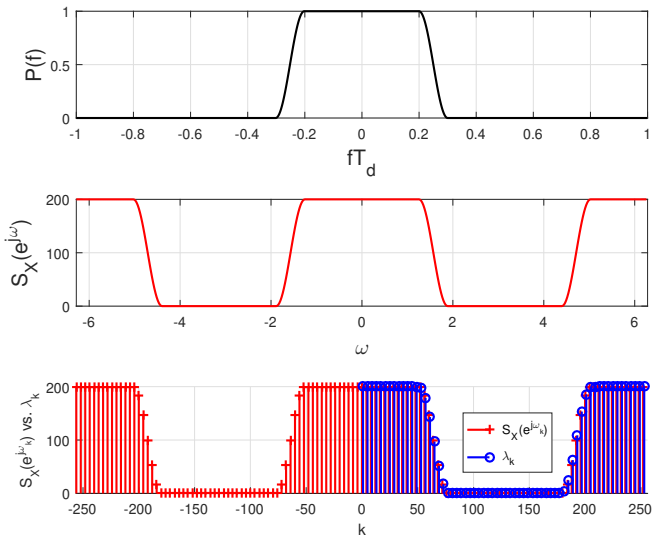

Fig. 19. (a) Raised cosine spectrum; (b) $S_X(e^{j\omega})$; (c) $S_X(e^{j\omega_k})$ versus eigenvalues λ_k

When $LT_d \to \infty$, $\Phi(\tau) \approx \sum_{l=-\infty}^{\infty} \Phi(\tau + lLT_d)$.
$\mathbf{\Phi}$ is a circulant matrix.
Hence, $\lambda_l \approx S_X(e^{j\omega_k}) = \sum_{l=0}^{L-1} \tilde{\Phi}(lT_d)e^{-j\omega_k l}$
$(l, k = 0, \ldots, L-1)$.
$\Rightarrow$ Transform from time domain to frequency domain!

- From the above decomposition, ISR in analog domain (see also Slide 15)

$$
\begin{aligned}
ISR_a = \frac{P_v}{P_z} &= \frac{\mathbf{h}^H(\mathbf{I}_L+\mu\mathbf{\Phi})^{-1}\mathbf{\Phi}(\mathbf{I}_L+\mu\mathbf{\Phi})^{-1}\mathbf{h}}{\mathbf{h}^H\mathbf{\Phi}\mathbf{h}} \\
&= \frac{\mathbf{h}^H\mathbf{F}(\mathbf{I}_L+\mu\mathbf{S}_X)^{-1}\mathbf{F}^{-1}\mathbf{F}\mathbf{S}_X\mathbf{F}^{-1}\mathbf{F}(\mathbf{I}_L+\mu\mathbf{S}_X)^{-1}\mathbf{F}^{-1}\mathbf{h}}{\mathbf{h}^H\mathbf{F}\mathbf{S}_X\mathbf{F}^{-1}\mathbf{h}} \\
&= \frac{\sum_{k=0}^{L-1}|H(e^{i\omega_k})|^2\frac{S_X(e^{j\omega_k})}{\left[1+\mu S_X(e^{j\omega_k})\right]^2}}{\sum_{k=0}^{L-1}|H(e^{i\omega_k})|^2 S_X(e^{j\omega_k})}
\end{aligned}
$$

- Similarly, ISR in digital domain $ISR_d = \dfrac{\sum_{k=0}^{L-1}|H(e^{j\omega_k})|^2\frac{S_{\tilde{X}}(e^{j\omega_k})}{\left[1+\mu S_X(e^{j\omega_k})\right]^2}}{\sum_{k=0}^{L-1}|H(e^{j\omega_k})|^2 S_{\tilde{X}}(e^{j\omega_k})}$,
  where $\tilde{X}(t) = X(t) * p^*(-t)$

- Denote $F_a(e^{j\omega}) = \frac{S_X(e^{j\omega})}{\left[1+\mu S_X(e^{j\omega})\right]^2}$ and $F_d(e^{j\omega}) = \frac{S_{\tilde{X}}(e^{j\omega})}{\left[1+\mu S_X(e^{j\omega})\right]^2}$

$$\begin{aligned}\overline{ISR}_a &= \frac{E_h\{P_v\}}{E_h\{P_z\}} = \frac{\sum_{k=0}^{L-1} E_h\left\{|H(e^{j\omega_k})|^2\right\} \frac{S_X(e^{j\omega_k})}{\left[1+\mu S_X(e^{j\omega_k})\right]^2}}{\sum_{k=0}^{L-1} E_h\left\{|H(e^{j\omega_k})|^2\right\} S_X(e^{j\omega_k})}, \\ &= \frac{\sum_{k=0}^{L-1} \frac{S_X(e^{j\omega_k})}{\left[1+\mu S_X(e^{j\omega_k})\right]^2}}{\sum_{k=0}^{L-1} S_X(e^{j\omega_k})}\end{aligned} \tag{19}$$

$$\begin{aligned}\overline{ISR}_d &= \frac{E_h\{P_{\tilde{V}}\}}{E_h\{P_{\tilde{Z}}\}} = \frac{\sum_{k=0}^{L-1} E_h\left\{|H(e^{j\omega_k})|^2\right\} \frac{S_{\tilde{X}}(e^{j\omega_k})}{\left[1+\mu S_X(e^{j\omega_k})\right]^2}}{\sum_{k=0}^{L-1} E_h\left\{|H(e^{j\omega_k})|^2\right\} S_{\tilde{X}}(e^{j\omega_k})} \\ &= \frac{\sum_{k=0}^{L-1} \frac{S_{\tilde{X}}(e^{j\omega_k})}{\left[1+\mu S_X(e^{j\omega_k})\right]^2}}{\sum_{k=0}^{L-1} S_{\tilde{X}}(e^{j\omega_k})}\end{aligned} \tag{20}$$

- Performance bounds:

$$ISRLB_a = \overline{ISR}_a|_{L\to\infty} = \frac{\frac{1}{2\pi}\int_0^{2\pi} \frac{S_X(e^{j\omega})}{\left[1+\mu S_X(e^{j\omega})\right]^2} d\omega}{\frac{1}{2\pi}\int_0^{2\pi} S_X(e^{j\omega}) d\omega}$$

$$= \frac{1+\beta(\sqrt{a+1}-1)}{(1+a)^2}$$

$$ISRLB_d = \overline{ISR}_d|_{L\to\infty} = \frac{\frac{1}{2\pi}\int_0^{2\pi} \frac{S_{\tilde{X}}(e^{j\omega})}{\left[1+\mu S_X(e^{j\omega})\right]^2} d\omega}{\frac{1}{2\pi}\int_0^{2\pi} S_{\tilde{X}}(e^{j\omega}) d\omega}$$

$$= \frac{1+\beta\left[\frac{2(a+1)^2}{a^2}\left(1-\frac{1}{\sqrt{a+1}}-\frac{a\sqrt{a+1}}{2(a+1)^2}\right)-1\right]}{(1+a)^2(1-\beta/4)}$$

where $a = \mu\frac{V_X^2 T_s}{K_1 K_2 T_d}$

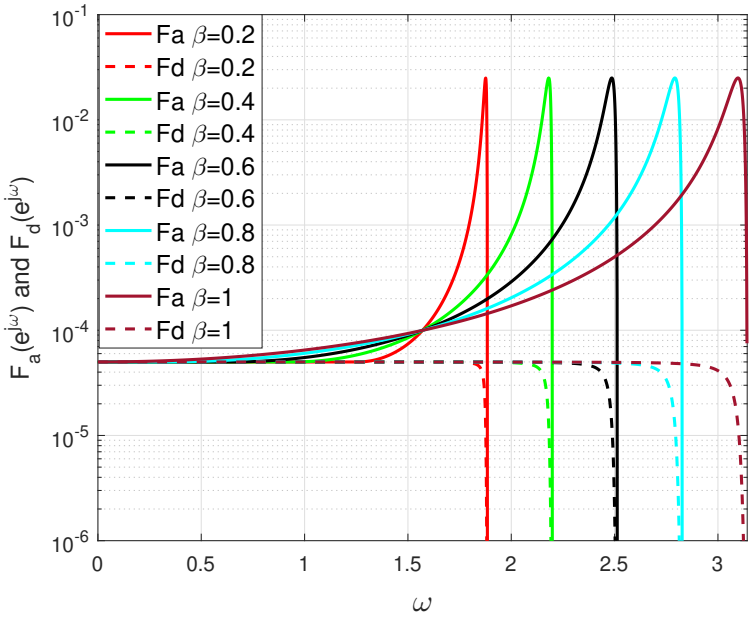

Fig. 20. Frequency dependent attenuation factors with various values of β.

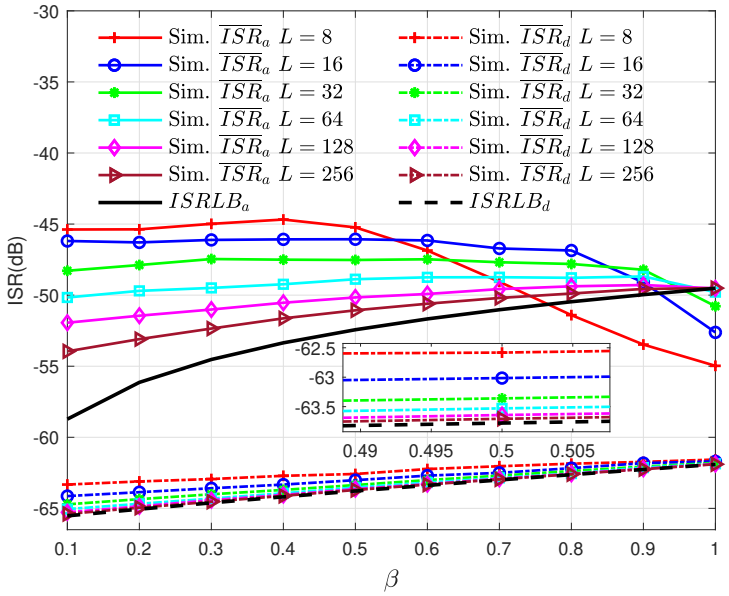

Fig. 21. ISRs in the analog domain and digital domain versus β.

- The peak is caused by $F_a(e^{j\omega})$
- The matched filter removes this peak (no peak seen in $F_d(e^{j\omega})$

- ISRLBs are derived for system design;
- The roles of β, loop gain, T_d, and L are revealed.

Outcome: One paper published in Transaction on Communications [J2]

3. ALMS Loop with I/Q Imbalances

- Since the ALMS loop is a quadrature based structure, I/Q imbalances in its modulators and demodulators may have a significant impact.
- Due to I/Q imbalance, the reference signal presented in the demodulator $(x_1(t))$ and modulator $(x_2(t))$ are:

$$x_i(t) = \frac{1+\rho_i e^{-j\theta_i}}{2} X(t) e^{j2\pi f_c t} + \frac{1-\rho_i e^{j\theta_i}}{2} X^*(t) e^{-j2\pi f_c t},$$
$$i = 1, 2$$

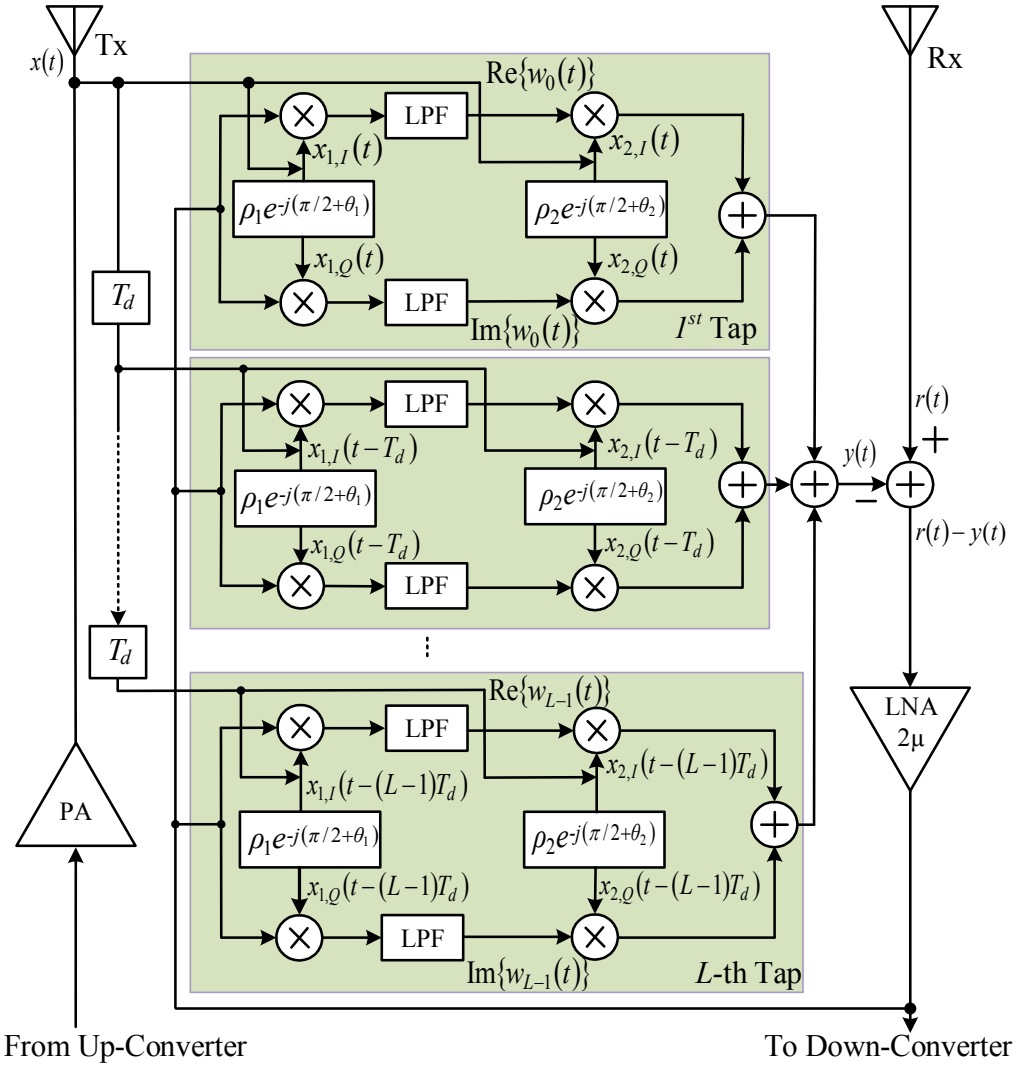

Fig. 22. ALMS loop with I/Q imbalances.

3. ALMS Loop with I/Q Imbalances

Impact on the loop gain:

- The loop gain with no I/Q imbalance: $G = \frac{V_y}{V_d} = \frac{2\mu V_x^2}{K_1 K_2}$;
- I/Q imbalances lead to loop gain variance: $G' = \frac{1}{2}\sqrt{(1+\rho_1^2)(1+\rho_2^2)}G$

$\Rightarrow$ Compensate by changing the gain of the LNA.

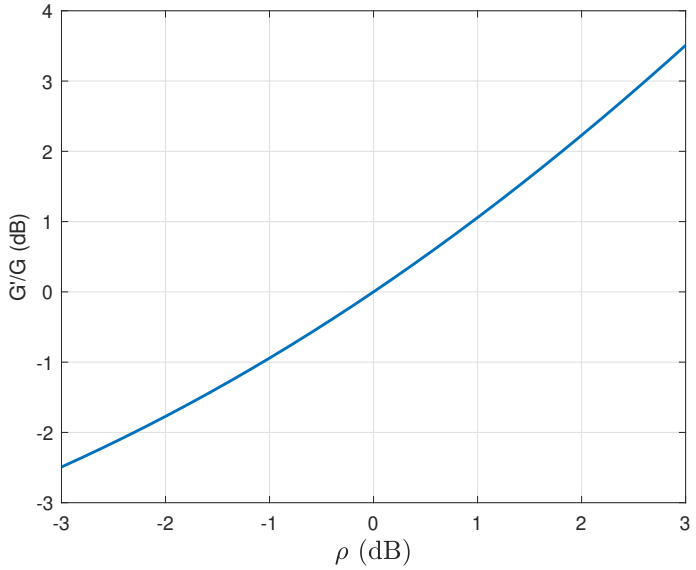

Fig. 23. The loop gain ratio versus amplitude.

3. ALMS Loop with I/Q Imbalances

Impact on the loop gain:

- The loop gain with no I/Q imbalance: $G = \frac{V_y}{V_d} = \frac{2\mu V_x^2}{K_1 K_2}$;
- I/Q imbalances lead to loop gain variance: $G' = \frac{1}{2}\sqrt{(1+\rho_1^2)(1+\rho_2^2)}G$

$\Rightarrow$ Compensate by changing the gain of the LNA.

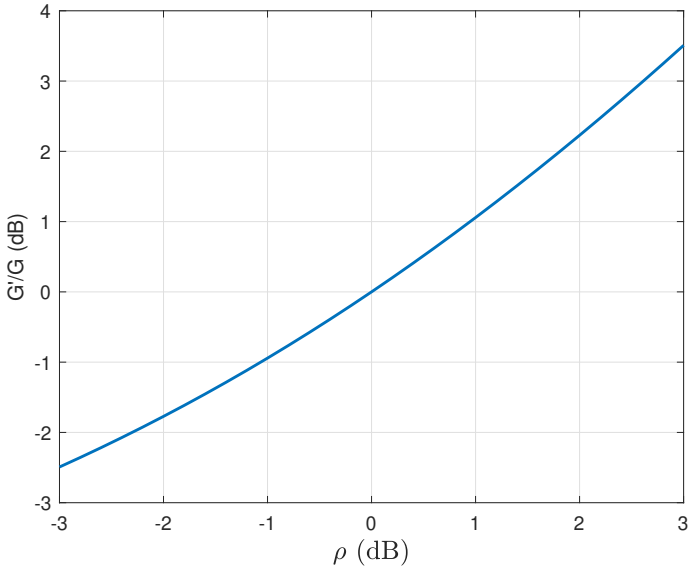

Fig. 23. The loop gain ratio versus amplitude.

Impact on the level of cancellation:

- The weighting error function under I/Q imbalance [J3, Appendix B]:

$$\bar{\bar{\mathbf{u}}} = \left[(\mathbf{I}_L + k_1\mathbf{\Phi}) - |k_2|^2\mathbf{E}\mathbf{\Phi}(\mathbf{I}_L + k_1^*\mathbf{\Phi})^{-1}\mathbf{E}^{-1}\mathbf{\Phi}\right]^{-1}\left[\mathbf{h} - k_2\mathbf{E}\mathbf{\Phi}(\mathbf{I}_L + k_1^*\mathbf{\Phi})^{-1}\mathbf{h}^*\right] \quad (21)$$

where $k_i = f(\rho_i, \theta_i), \mathbf{E} = diag\{1, \cdots, e^{j4\pi f_c(L-1)T_d}\}$

3. ALMS Loop with I/Q Imbalances

- Note if no I/Q imbalance $k_1 = \mu$, $k_2 = 0$, thus $\bar{\bar{\mathbf{u}}} = (\mathbf{I}_L + \mu\mathbf{\Phi})^{-1}\mathbf{h}$
- In both cases, normalised RI power follows (see also Eq.(9))

$$P_{RI}(t) = \frac{1}{K_1 K_2}\bar{E}\{|z(t) - y(t)|^2\} = \frac{1}{2}\bar{\bar{\mathbf{u}}}^H \mathbf{\Phi}\bar{\bar{\mathbf{u}}} \tag{22}$$

- The level of cancellation is degraded due to I/Q imbalance as

$$\begin{aligned} DF &= 10\log_{10}\frac{P_d}{P_0} = 10\log_{10}\left[\frac{\text{RI power (with I/Q)}}{\text{RI power (without I/Q)}}\right] \\ &= 10\log_{10}\frac{\bar{\bar{\mathbf{u}}}^H \mathbf{\Phi}\bar{\bar{\mathbf{u}}}}{\mathbf{h}^H \mathbf{Q}\text{diag}\left\{\frac{\lambda_l}{(1+\mu\lambda_l)^2}\right\}\mathbf{Q}^{-1}\mathbf{h}} \end{aligned} \tag{23}$$

3. ALMS Loop with I/Q Imbalances

- Averaging degradation factor over SI channel: $\overline{DF} = 10\log_{10}\frac{E_h\{P_d\}}{E_h\{P_0\}}$
- DF upper bound: $DF_u = 20\log_{10}\frac{(1+\rho^2)\left(1+\rho^2+\sqrt{1-2\rho^2\cos 2\theta+\rho^4}\right)}{4\rho^2\cos^2\theta}$

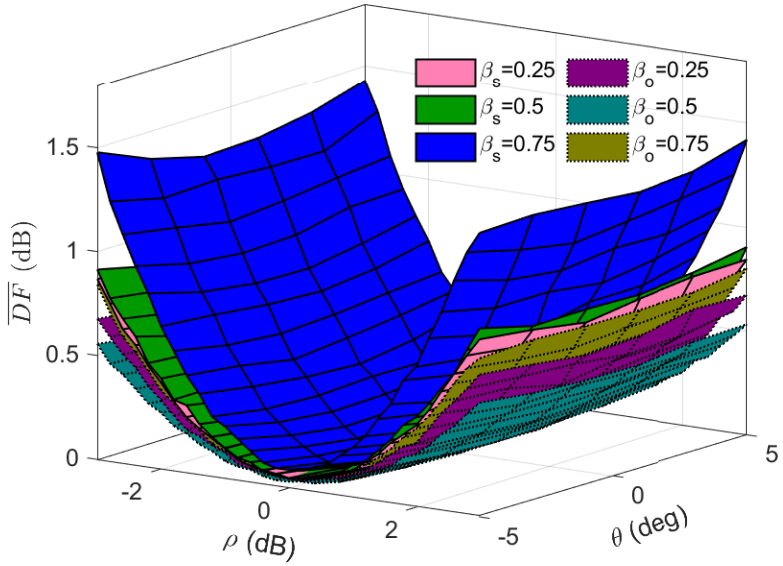

Fig. 24. $\overline{DF}$ vs. amplitude and phase errors with different β [J3, Fig. 4b].

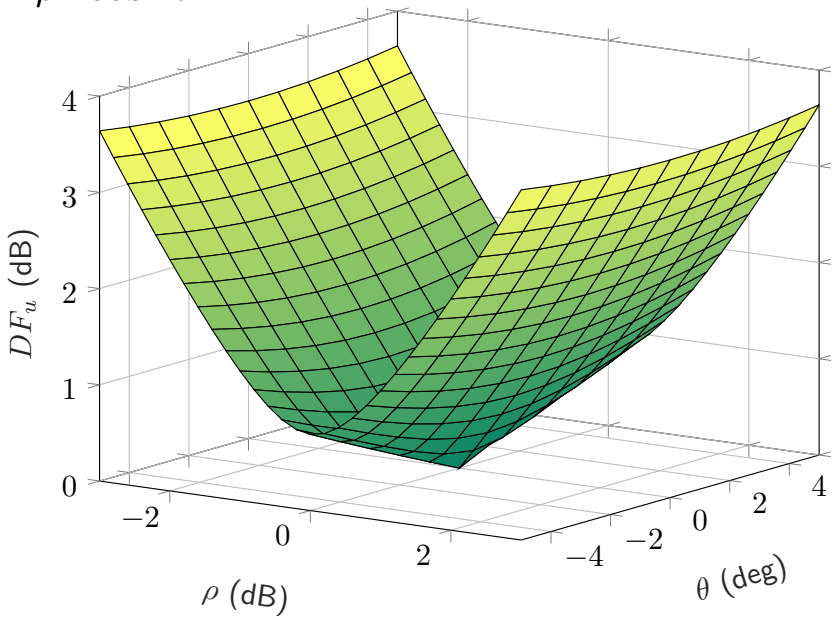

Fig. 25. Upper bound of DF vs. amplitude and phase errors [J3, Fig. 6]

3. ALMS Loop with I/Q Imbalances

- Averaging degradation factor over SI channel: $\overline{DF} = 10\log_{10}\frac{E_h\{P_d\}}{E_h\{P_0\}}$
- DF upper bound: $DF_u = 20\log_{10}\frac{(1+\rho^2)\left(1+\rho^2+\sqrt{1-2\rho^2\cos 2\theta+\rho^4}\right)}{4\rho^2\cos^2\theta}$

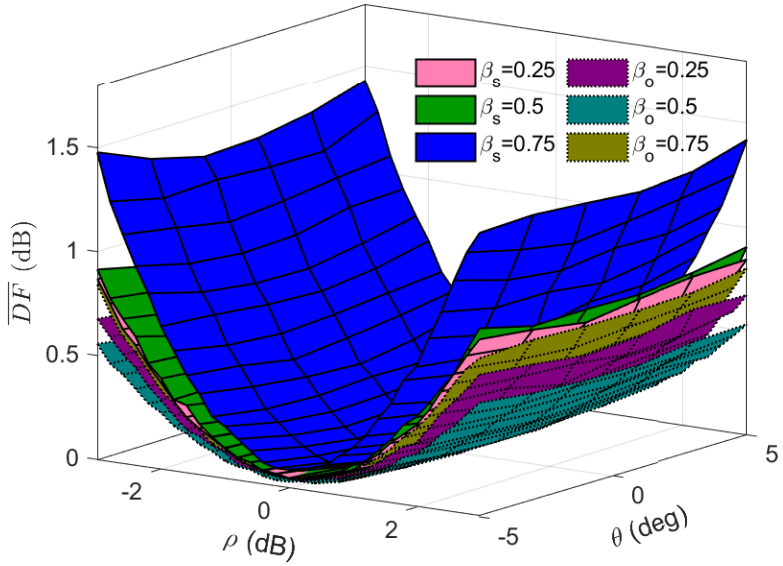

Fig. 24. $\overline{DF}$ vs. amplitude and phase errors with different β [J3, Fig. 4b].

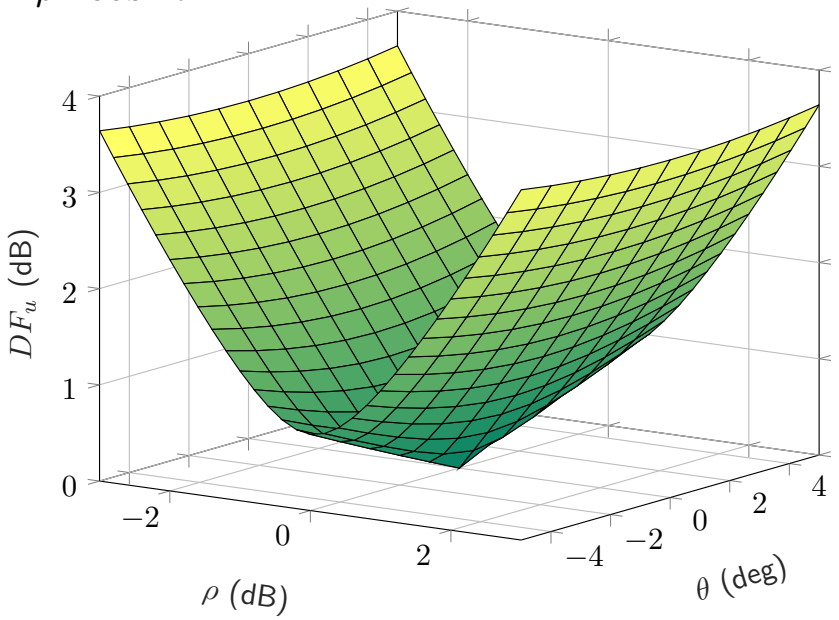

Fig. 25. Upper bound of DF vs. amplitude and phase errors [J3, Fig. 6]

Findings:

- ALMS loop is resilient to I/Q imbalances (usually $\leqslant 1.5$ dB, 3.5 dB max)
- DF_u determines level of compensation required in other domains.

Outcome: A paper published in Transactions on Vehicular Technology [J3].

4. Challenges of SIC for MIMO Systems

Research problems:

- Great complexity of SIC for IBFD MIMO: # analog cancellation circuits $= M^2$
- Complexity of DSP for tuning weights: M^2;

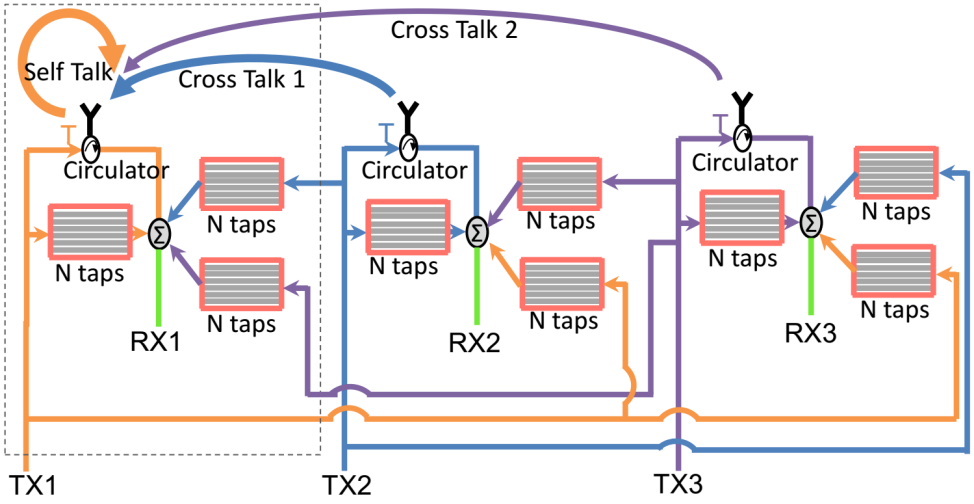

Fig. 26. Complexity of SIC in IBFD MIMO [3].

[3]D. Bharadia and S. Katti, "Full duplex MIMO radios," in Proceedings of the 11th USENIX Conference on Networked Systems Design and Implementation, ser. NSDI'14.

$\Rightarrow$ How to adopt the ALMS loop for MIMO systems with low complexity?

Proposed Beam-based Analog SIC

Signal models:

- Transmitted signals: $\mathbf{X}(t) = \mathbf{A}\mathbf{S}(t)$

  $\mathbf{X}(t) = [X_1(t), \cdots, X_N(t)]^T$,

  $\mathbf{S}(t) = [S_1(t), \cdots, S_K(t)]^T$,

  $S_k(t) = \sum_{i=-\infty}^{\infty} s_k(i)p(t - iT_s)$, and

  $\mathbf{A}$ is the beamforming matrix.

- SI signals at M receive antennas:

  $\mathbf{Z}(t) = \sum_{l=0}^{L-1} \mathbf{H}^H(l)\mathbf{A}\mathbf{S}(t - lT_d)$

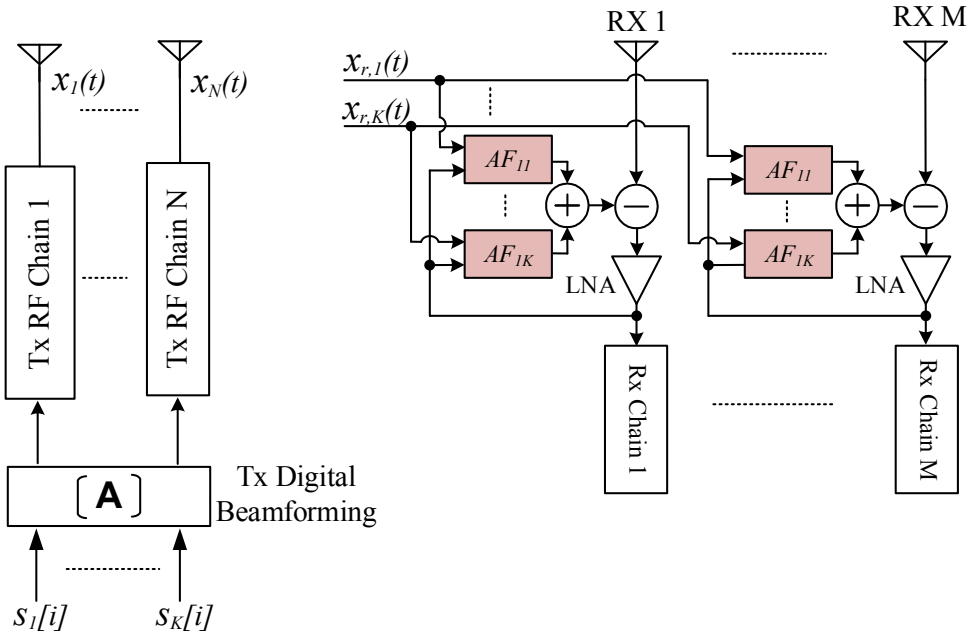

Fig. 27. Proposed beam-based analog SIC.

Proposed Beam-based Analog SIC

Signal models:

- Transmitted signals: $\mathbf{X}(t) = \mathbf{A}\mathbf{S}(t)$

  $\mathbf{X}(t) = [X_1(t), \cdots, X_N(t)]^T$,

  $\mathbf{S}(t) = [S_1(t), \cdots, S_K(t)]^T$,

  $S_k(t) = \sum_{i=-\infty}^{\infty} s_k(i)p(t - iT_s)$, and

  $\mathbf{A}$ is the beamforming matrix.

- SI signals at M receive antennas:

  $\mathbf{Z}(t) = \sum_{l=0}^{L-1} \mathbf{H}^H(l)\mathbf{A}\mathbf{S}(t - lT_d)$

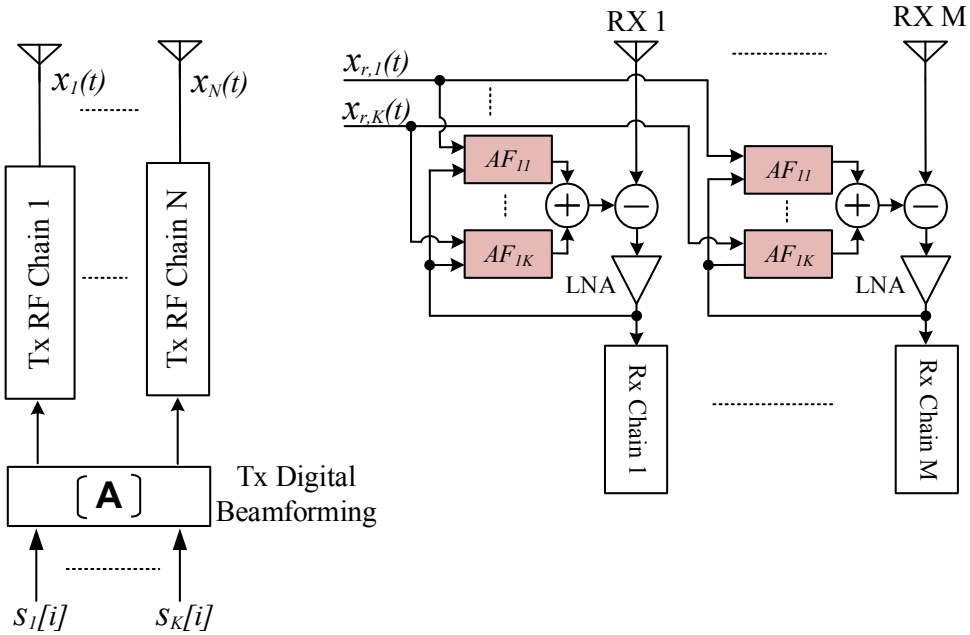

Fig. 27. Proposed beam-based analog SIC.

Beam-based analog SIC:

- $\mathbf{Z}(t)$ is a linear transformation of beam signals $\mathbf{S}(t)$.
- Cancellation signal should be: $\mathbf{y}(t) = \text{Re}\{\sum_{l=0}^{L-1} \mathbf{W}^H(l,t)\mathbf{x}_r(t - lT_d)\}$,
  where $\mathbf{x}_r(t) = [x_{r,1}(t), \ldots, x_{r,K}(t)]$ generated from $\mathbf{s}_k(i), k = 1, \cdots, K$
- Since $K \ll N$, the number of adaptive filters are significantly reduced.

Beam-based Analog SIC with Additional Tx Chains

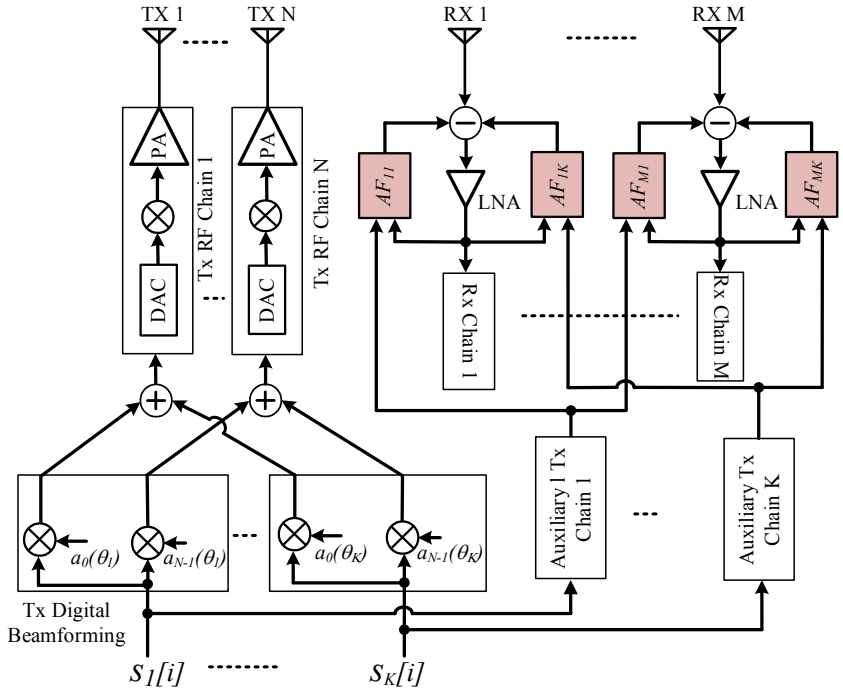

Fig. 28. Beam-based analog SIC with additional Tx chains.

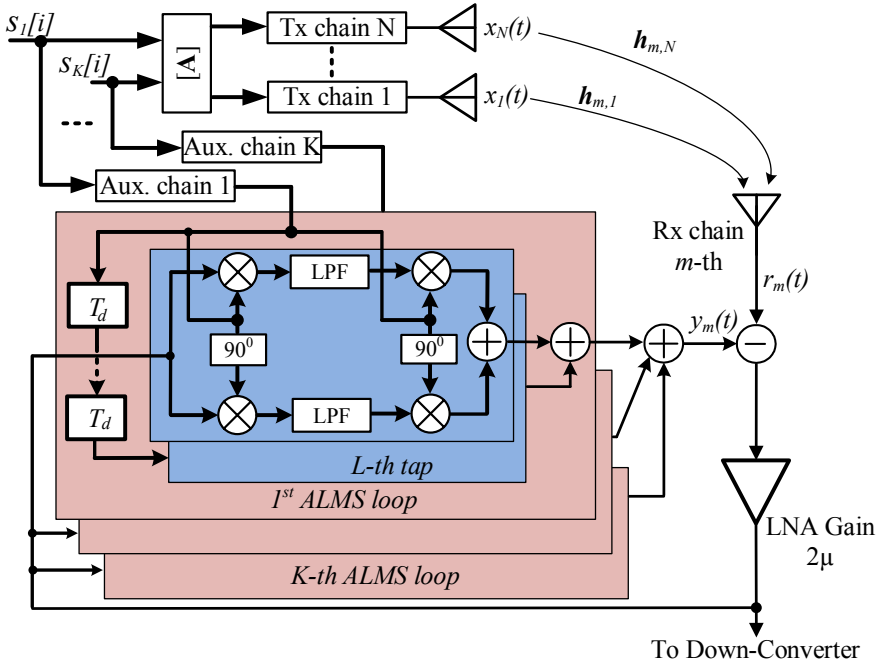

Fig. 29. K ALMS loop at m-th receiver chain.

Interference suppression ratio: $ISR = \dfrac{\underline{\mathbf{h}}^H \mathbf{Q} \mathrm{diag}\left\{ \dfrac{\lambda_i}{(1+\mu\lambda_i)^2} \right\} \mathbf{Q}^{-1} \underline{\mathbf{h}}}{\underline{\mathbf{h}}^H \mathbf{Q} \mathrm{diag}\{\lambda_i\} \mathbf{Q}^{-1} \underline{\mathbf{h}}}$

where $\underline{\mathbf{h}} = [\mathbf{I}_M \otimes (\mathbf{A}^H \otimes \mathbf{I}_L)]\mathbf{h}$ and $\lambda_i, i = 1, \cdots, M \times K \times L$ are eigenvalues of the matrix $\mathbf{\Psi} = \mathbf{I}_{MK} \otimes \mathbf{\Phi}$.

Beam-based Analog SIC with Additional Tx Chains

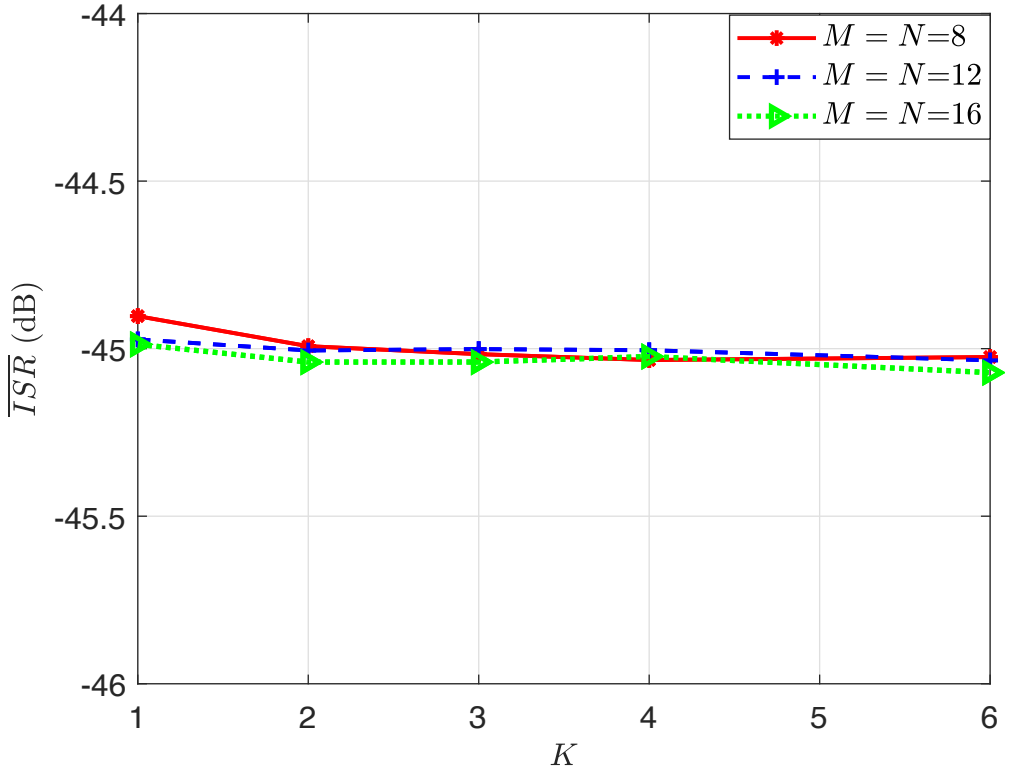

Fig. 30. The averaged and converged interference suppression ratio.

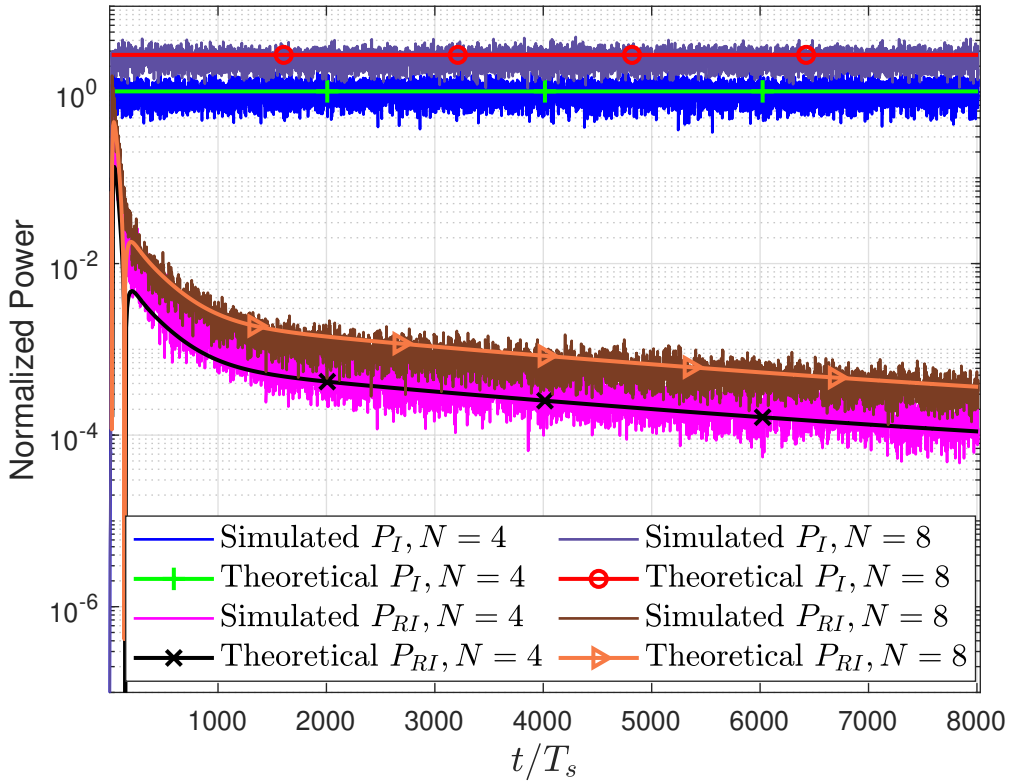

Fig. 31. Normalized SI and residual SI powers for 2 beams FD MIMO systems.

$\Rightarrow$ The performance of SIC depends on ALMS loop rather than the number of beams and transmit and receive antennas.

Outcome: Conference paper presented in SPAWC 2019 [C3]

Beam-based Analog SIC: Dig It Deeper

- Additional transmit chains: **still complex!!**
- Further reduce complexity: Choosing K reference signals from N transmit signals - **Generalised Beam-based Analog SIC**

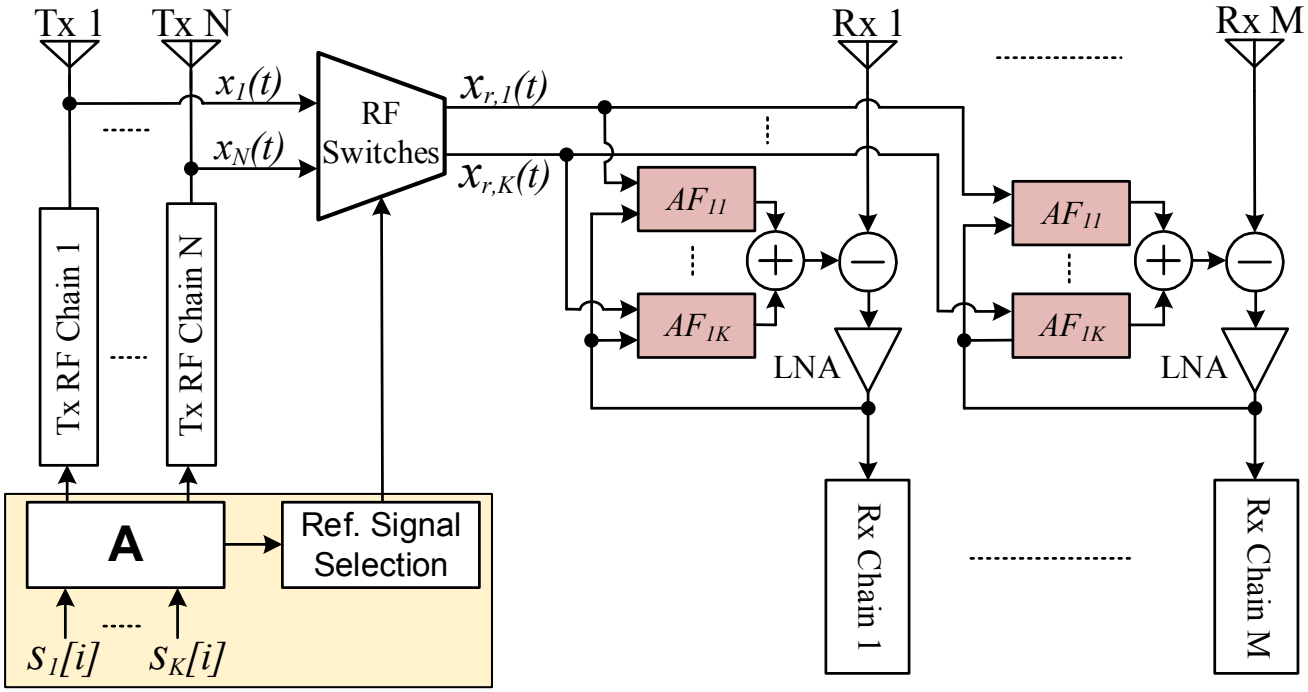

Fig. 32. Proposed beam-based analog SI cancellation structure.

Beam-based Analog SIC: Dig It Deeper

Interference suppression ratio:

$$ISR = \frac{\epsilon^2 + \bar{\bar{\mathbf{u}}}^H [\mathbf{I}_M \otimes \mathbf{\Theta}] \bar{\bar{\mathbf{u}}}}{\epsilon^2 + \underline{\mathbf{h}}^H [\mathbf{I}_M \otimes \mathbf{\Theta}] \underline{\mathbf{h}}} \tag{24}$$

where $\bar{\bar{\mathbf{u}}} = \mathbf{Q}\text{diag}\left\{\frac{1}{1+\mu\lambda_i}\right\}\mathbf{Q}^{-1}\underline{\mathbf{h}}$, and $\lambda_i, i = 1, \cdots, MKL$ are the eigenvalues of the matrix $\mathbf{\Psi} = \mathbf{I}_M \otimes \left[(\mathbf{B} \otimes \mathbf{I}_L)\mathbf{\Theta}\right] = \mathbf{I}_M \otimes \left[(\mathbf{B} \otimes \mathbf{I}_L)(\mathbf{I}_K \otimes \mathbf{\Phi})\right]$ with $\mathbf{B} = \mathbf{A}_r^H \mathbf{A}_r$ and $\mathbf{A}_r \subset \mathbf{A}$.

- When $M = N = K = 1$, i.e., single antenna system, (24) becomes [1,Eq. (39)] (see also Slide 15);
- When $\mathbf{B} = \mathbf{I}_K$, $\mathbf{\Psi} = \mathbf{I}_{MK} \otimes \mathbf{\Phi}$ i.e., additional Tx chains are employed (see Slide 37).

$\Rightarrow$ This is a generalized structure of employing the ALMS loop.

Beam-based Analog SIC: Dig It Deeper

Proposed Reference Signal Selection Method:

- From $\bar{\bar{\mathbf{u}}} = \mathbf{\Omega}\underline{\mathbf{h}}$, $(\mathbf{\Omega} = \mathbf{Q}\text{diag}\left\{\frac{1}{1+\mu\lambda_i}\right\}\mathbf{Q}^{-1})$, $\mathbf{\Omega}$ is the transform matrix of vector $\underline{\mathbf{h}}$.
- Det($\mathbf{\Omega}$) is the scaling factor of this transformation
- $\mathbf{A}_r$ is found if it gives the maximum $D_{\mathbf{\Omega}} = |\prod_{i=1}^{M\times K\times L}(1+\mu\lambda_i)|$

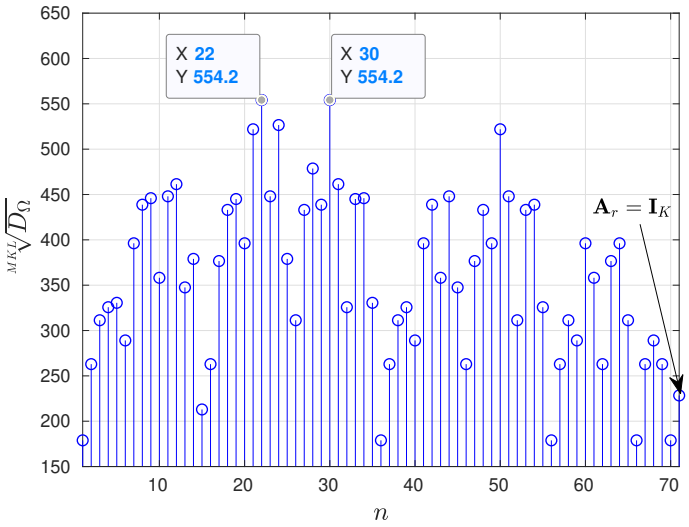

Fig. 33. Geometric mean of D_Ω.

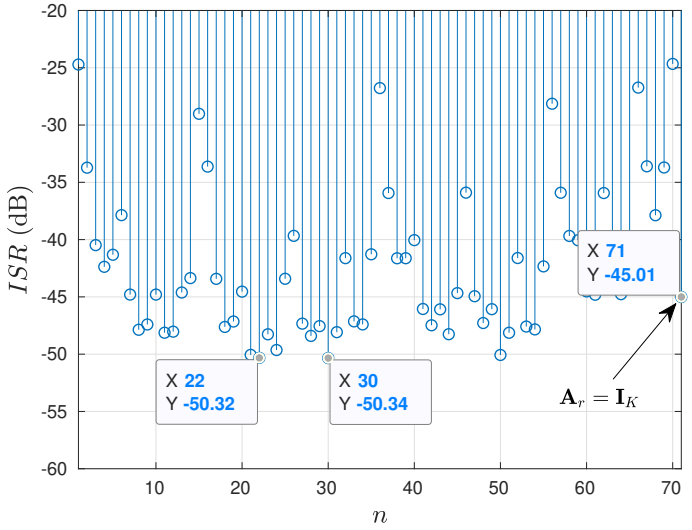

Fig. 34. ISR for all possible selections of $\mathbf{A}_r$.

Beam-based Analog SIC: Dig It Deeper

Simulation results:

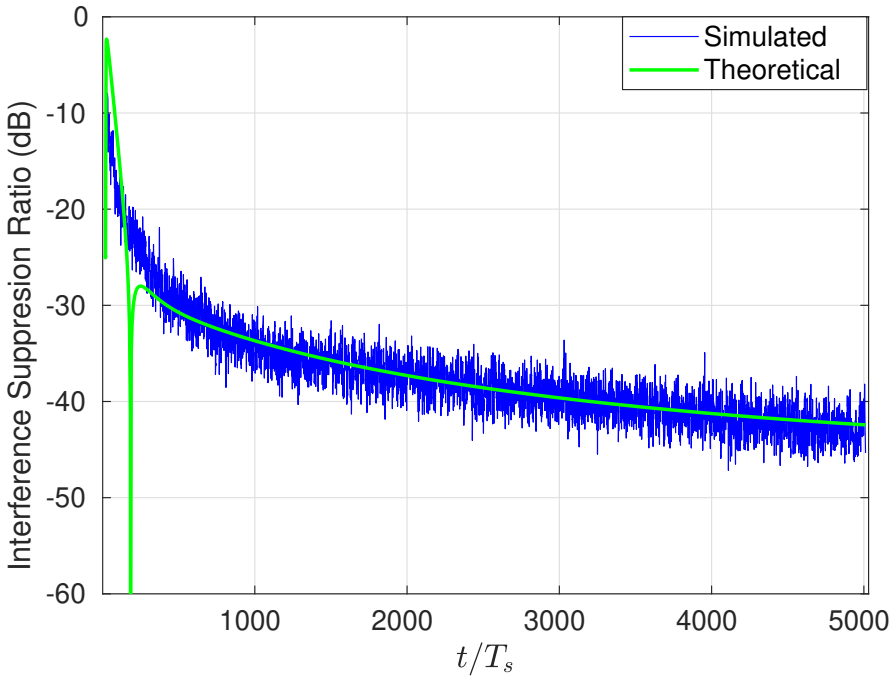

Fig. 35. Interference suppression ratio for $N = M = 8, K = 4$, T_d spaced SI channels.

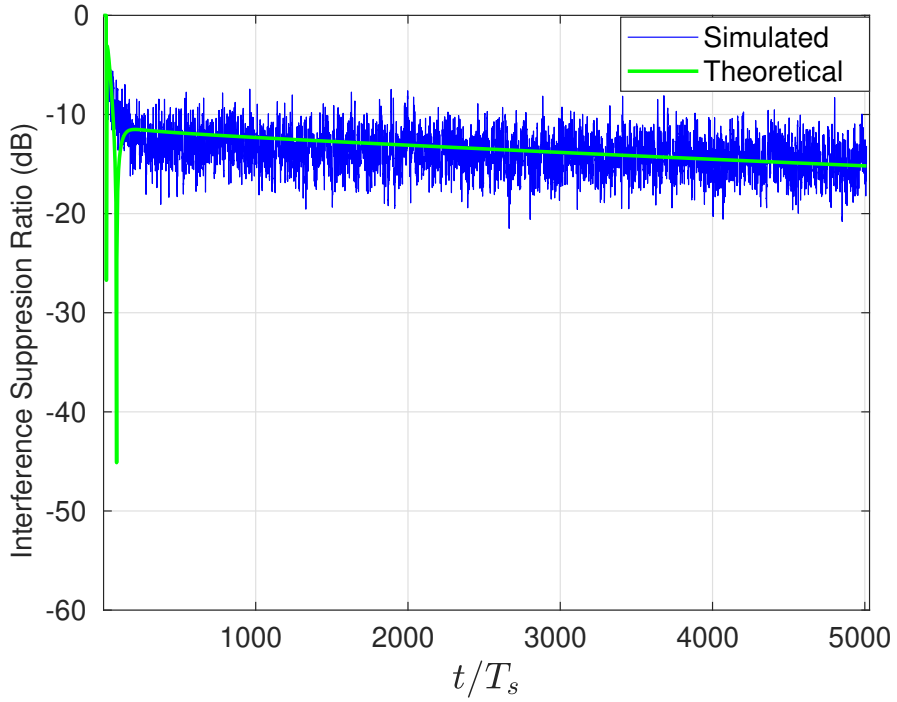

Fig. 36. Interference suppression ratio with the worst reference signals.

Outcome: A paper submitted to TWC (under review - 2nd round) [J4]

ALMS Loop - A Practical Perspective

- Measurement results are necessary to validate these findings;
- Implementation of the ALMS loop is challenging due to lack of high gain RF multipliers.

⇒ Proposed: quadrature modulator and demodulator combined with variable gain amplifier to replace ideal RF multipliers.

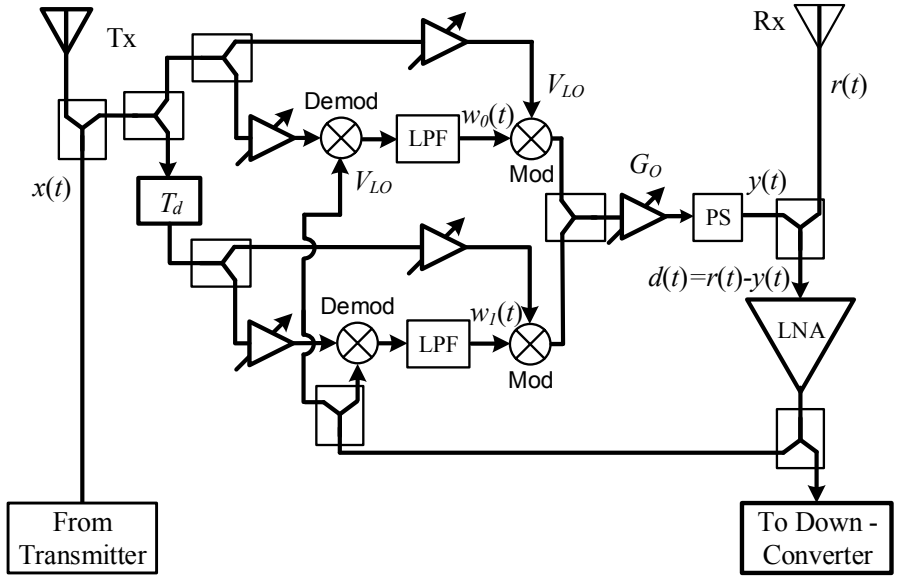

Fig. 37. Proposed practical ALMS loop with two taps.

ISR is expected as:

$$ISR \leqslant \frac{(1+a')^2}{1+\beta(\sqrt{a'+1}-1)} \qquad (25)$$

where $a' = G\frac{T_s}{T_d}$ and $G = \mu\frac{V_{LO}^2}{K_1 K_2} G_O$.

Prototype of ALMS Loop

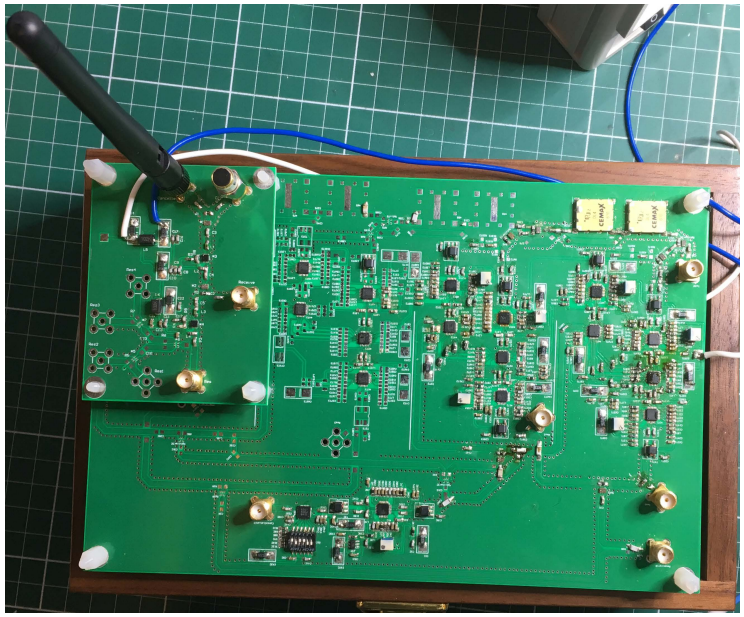

Fig. 38. A prototype of the ALMS loop.

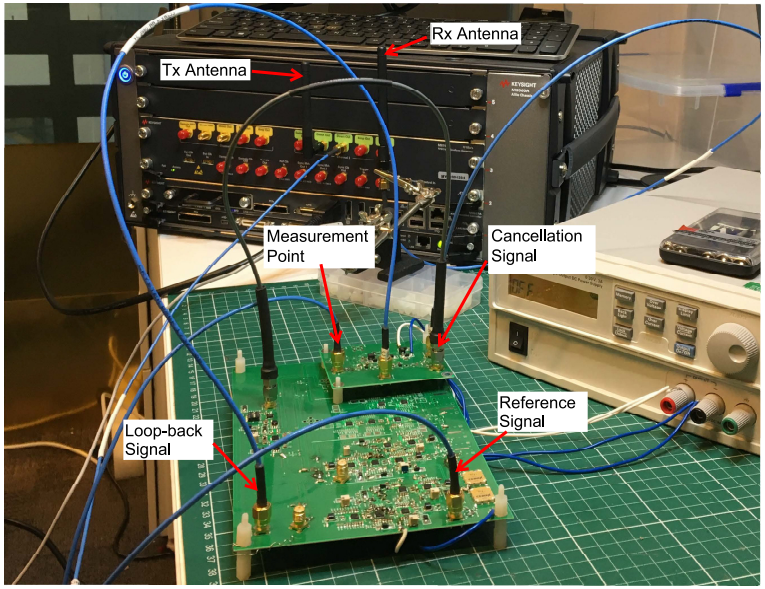

Fig. 39. Test setup.

Detail components:

- Delay line: DL4 (4 ns)
- Mod/Demod: ADL5373 & ADL5382
- Power splitter: Anaren PD2328J5050S2HF
- Variable gain amplifier: ADL5330

- Transmitter: Keysight M8190A, 2.4 GHz carrier frequency
- Transmit power: -7.75 dBm
- Tx to Rx antenna: 75 mm

Receiver: power combiner, LNA, and spectrum analyzer.

Performance with Different Bandwidths

20 MHz Bandwidth ($T_s = 62.5$ ns):
From (25), ISR $\approx$ 42 dB
Measured: 39 dB

50 MHz Bandwidth ($T_s = 25$ ns):
From (25), ISR $\approx$ 36 dB
Measured: 33 dB

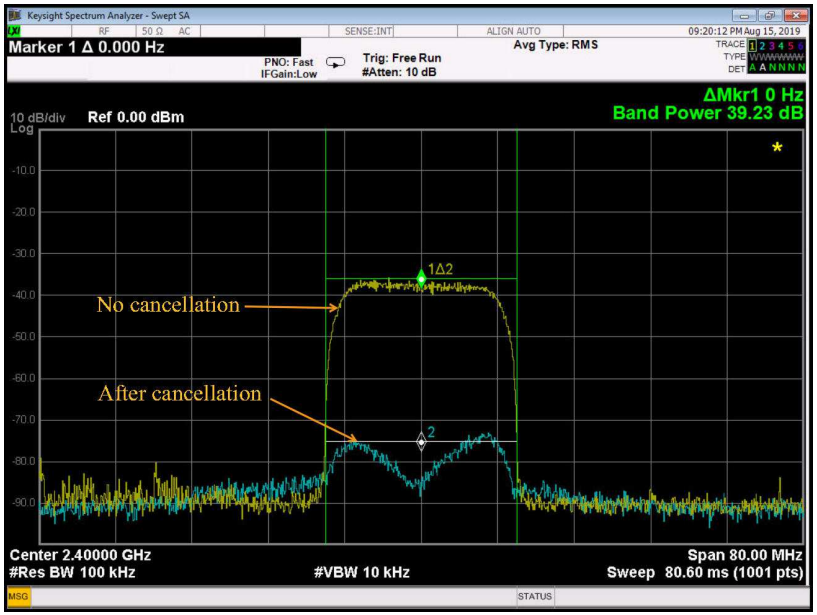

Fig. 40. 20 MHz bandwidth.

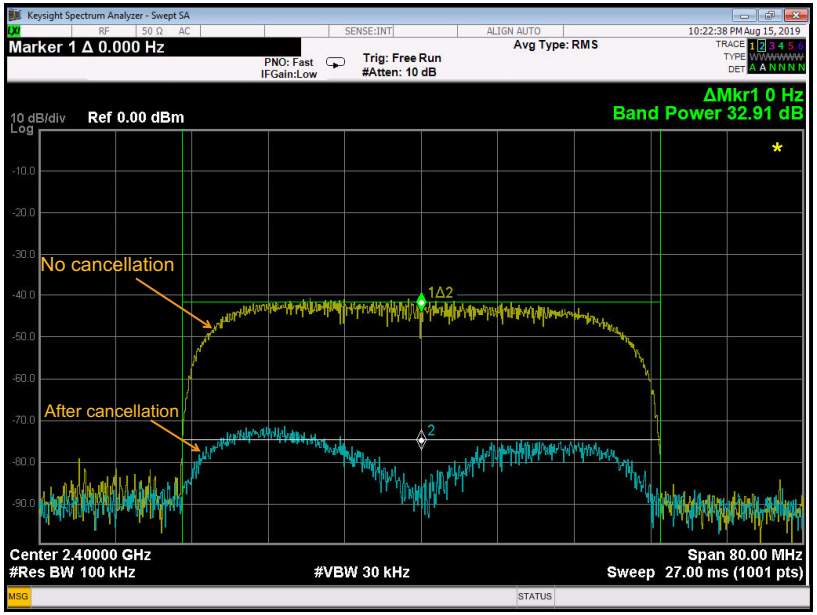

Fig. 41. 50 MHz bandwidth.

$\Rightarrow$ Measurement results are justifiable with the expectations!!

Performance with Different Signal Properties

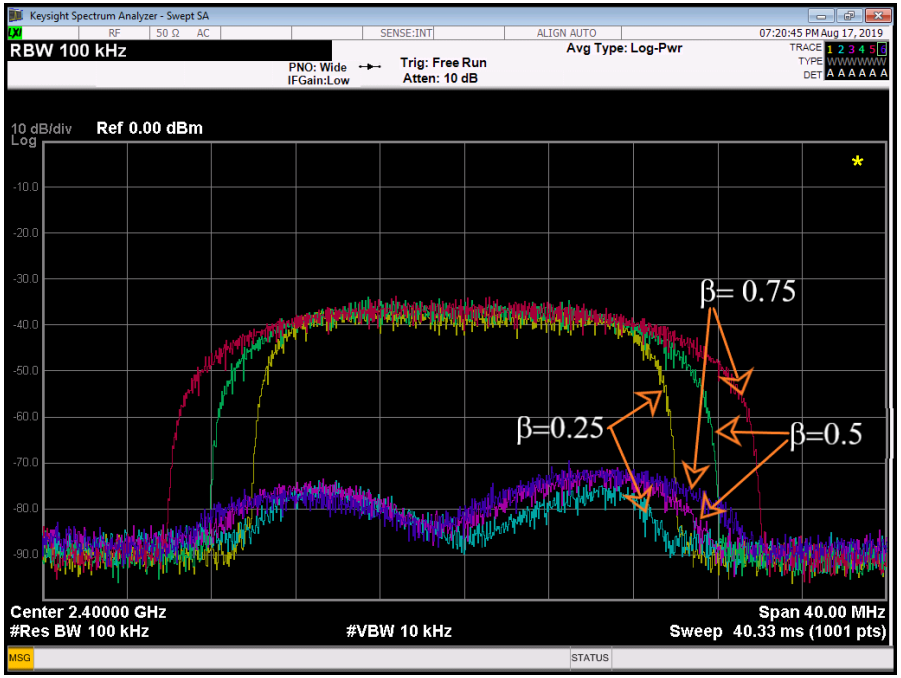

Fig. 42. Cancellation performances with different roll-off factors.

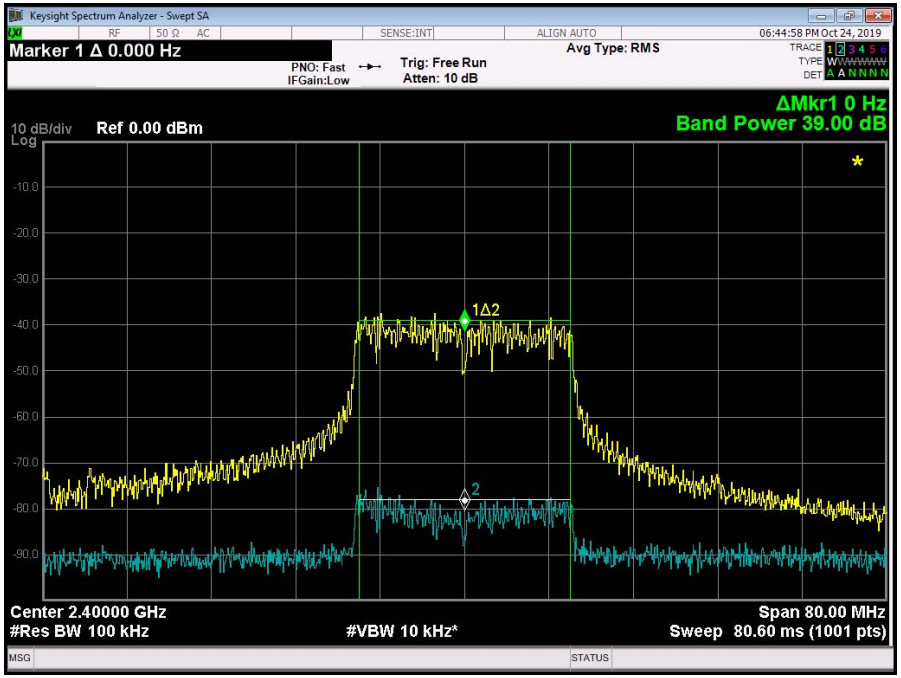

Fig. 43. Cancellation performances with OFDM signal.

These results confirm the above theoretical analyses. Outcome: One paper presented in ITNAC 2019 [C4] and an extended version is submitted to Sensors [J5].

List of Publications

Journals

[J1] A. T. Le, L. C. Tran and X. Huang, "Cyclostationary Analysis of Analog Least Mean Square Loop for Self-Interference Cancellation in In-Band Full-Duplex Systems", *IEEE Commun. Letters*, Dec. 2017

[J2] A. T. Le, L. C. Tran, X. Huang, Y. Jay Guo, and J. Yiannis C. Vardaxoglou, "Frequency Domain Characterization and Performance Bounds of ALMS Loop for RF Self-Interference Cancellation", *IEEE Trans. Commun.*, Jan. 2019.

[J3] A. T. Le, L. C. Tran, X. Huang, and Y. Jay Guo, "Analog Least Mean Square Loop With I/Q Imbalance for Self-Interference Cancellation in Full-Duplex Radios", *IEEE Trans. Vehicular Technol.*, Oct. 2019.

[J4] A. T. Le, L. C. Tran, X. Huang, and Y. Jay Guo, "Beam-Based Analog Self-Interference Cancellation in Full-Duplex MIMO Systems", *Submitted to IEEE Trans. Wireless Commun.*

[J5] A. T. Le, L. C. Tran, X. Huang, and Y. Jay Guo, "Beam-Based Analog Self-Interference Cancellation in Full-Duplex MIMO Systems", *Submitted to Sensors.*

List of Publications

Conferences

[C1] A. T. Le, L. C. Tran and X. Huang, "On Performance of Analog Least Mean Square Loop for Self-Interference Cancellation in In-Band Full-Duplex OFDM Systems", *IEEE 85th Vehicular Technology Conference (VTC Spring)*, Sydney, Australia, 2017.

[C2] A. T. Le, Y. Nan, L. C. Tran, X. Huang, J. Gou and Y. Vardaxoglou, "Self-Interference Cancellation for Generalized Continuous Wave SAR", *IEEE 87th Vehicular Technol. Conf. (VTC Fall)*, Chicago, USA, 2018.

[C3] A. T. Le, L. C. Tran, X. Huang, and Y. Jay Guo, Beam-Based Analog Self-Interference Cancellation with Auxiliary Transmit Chains in Full-Duplex MIMO Systems, *IEEE 20th Inter. Workshop Signal Processing Advances in Wireless Commun. (SPAWC)*, Cannes, France, 2019.

[C4] A. T. Le, L. C. Tran, X. Huang, and Y. Jay Guo, Analog Least Mean Square Loop for Self-Interference Cancellation: Implementation and Measurements, *29th Inter. Telecommun. Networks and Applications Conf. (ITNAC)*, Aukland, New Zealand, 2019.

Conclusions

- The properties of the ALMS loop have been comprehensively investigated;
- The performances of the ALMS loop in different IBFD systems have been analysed.
- A novel analog SIC structure using the ALMS loop for IBFD MIMO has been proposed.
- A practical structure and a prototype of the ALMS loop has been developed to provide experimental results.

$\Rightarrow$ **The ALMS loop is a promising structure for SIC in any IBFD systems.**

Future work:

- Applying the ALMS algorithm to other applications
- Developing a complete IBFD system